frontiers | Frontiers in Mechanical Engineering

TYPE Review
PUBLISHED 04 April 2024
DOI 10.3389/fmech.2024.1357087



OPEN ACCESS

EDITED BY
Mohammad Arefi,
University of Kashan, Iran

REVIEWED BY
Chunhui Wang,
Xi'an Jiaotong University, China
Ahmed Mourtada Elseman,
Central Metallurgical Research and Development Institute (CMRDI), Egypt

*CORRESPONDENCE
Jayant Giri,
jayantpgiri@gmail.com

RECEIVED 17 December 2023
ACCEPTED 18 March 2024
PUBLISHED 04 April 2024

CITATION
Kumar S, Sharma SS, Giri J, Makki E, Sathish T and Panchal H (2024), Perovskite materials with improved stability and environmental friendliness for photovoltaics.
*Front. Mech. Eng* 10:1357087.
doi: 10.3389/fmech.2024.1357087



# Perovskite materials with improved stability and environmental friendliness for photovoltaics

Sujit Kumar[1], Sasanka Sekhor Sharma[2], Jayant Giri[3]*, Emad Makki[4,5], T. Sathish[6] and Hitesh Panchal[7]

[1]Department of Electrical and Electronics Engineering, Dayananda Sagar College of Engineering, Bengaluru, Karnataka, India, [2]Department of Electrical Engineering, Assam Engineering College, Assam Science and Technological University, Guwahati, Assam, India, [3]Department of Mechanical Engineering, Yeshwantrao Chavan College of Engineering, Nagpur, India, [4]Department of Mechanical Engineering, College of Engineering and Architecture, Umm Al-Qura University, Makkah, Saudi Arabia, [5]Department of Ocean and Resources Engineering, School of Ocean and Earth Science and Technology, University of Hawaii at Manoa, Honolulu, HI, United States, [6]Saveetha School of Engineering, SIMATS, Chennai, Tamil Nadu, India, [7]Department of Mechanical Engineering, Government Engineering College Patan, Patan, Gujarat, India

Finding innovative, stable, and environmentally acceptable perovskite (PVK) sunlit absorber constituents has developed a major area of study in photovoltaics (PVs). As an alternative to lead-based organic-inorganic halide PVKs, these PVKs are being researched for use in cutting-edge PVK solar cells. While there has been progress in this field as of late, there are still several scientific and technical questions that have yet to be answered. Here, we offer insights into the big picture of PVK toxicity/instability research, and then we discuss methods for creating stable, non-toxic PVKs from scratch. It is also believed that the processing of the proposed PVKs, which occurs between materials design and actual devices, poses novel challenges. PVK PVs that are both stable and ecologically benign can be created if these topics receive more attention. It is interesting to note that although perovskite solar cells (PSCs) have impressive power conversion efficiency, their commercial adoption is hindered by lead toxicity. Lead is a hazardous material that can cause harm to humans and the environment. As a result, researchers worldwide are exploring non-toxic lead-free photovoltaics (PSCs) for a sustainable and safe environment. To achieve this goal, lead in PSCs is replaced by non-toxic or less harmful metals such as tin, germanium, titanium, silver, bismuth, and copper. A study has been conducted that provides information on the characteristics, sustainability, and obstacles of replacing lead with these metals in PSCs. The paper also explores solutions for stability and efficiency issues in lead-free, non-toxic PSC commercialization, including altering manufacturing techniques and adding additives. Lastly, it covers the latest developments/future perspectives in lead-free perovskite solar cells that can be implemented in lead-free PSCs.

KEYWORDS

**perovskite, non-lead perovskite material, perovskite solar cells, chemical process, power conversion efficiency**

## 1 Introduction

Despite being the most plentiful, free, and sustainable energy source, traditional photovoltaics (PVs) are still more expensive than fossil fuels in most places (Gratzel, 2014; Green et al., 2014). This highlights the critical need for the rapid advancement of PVs of the subsequent group that are both extremely competent and suitably priced. In this context, perovskite (PVK) solar cells (PSCs) have developed as a revolutionary thin-film PV technology, rapidly reigniting research into the development of PVs (Liu et al., 2013; Jeon et al., 2014; Correa-Baena et al., 2017). The power conversion efficiency (PCE) of PSCs has climbed recklessly now up to 23% which has been shown in (Kojima et al., 2009; National Center for Photovoltaics, 2024).

The major light absorbers in PSCs are PVK-type materials. Since the earliest days of PSC research, lead-based organic-inorganic halide PVKs (OIHPs) (Kim et al., 2012; Zhou et al., 2016), with a typical chemical formula of $ABX_3$ (Kim et al., 2012; Zhou et al., 2016), have been the most explored PVKs. PVK absorber materials now include "low-dimensional" and chalcogenide PVKs (PCP) (Snaith, 2013; Cao et al., 2015; Tsai et al., 2016; Xiao et al., 2018). Perovskites are a class of extremely effective solar cells based on Pb halides. The most popular type is Pb-based organic-inorganic halide perovskites, which have the general formula $ABX_3$. Here A can be $CH_3NH_3$ + (MA+) or $HC(NH_2)_2$ + (FA+); B is $Pb^{2+}$; and X can be I, Br or Cl (shown in Figure 1). These perovskites are widely studied because of their high efficacy and low rate. They can be used in different forms, including thin films, quantum dots, and nanorods. However, the stability and degradation of perovskites are important issues that need.

Despite current research into alternate PVK materials, the B-site positive ion in modern PSCs is still lead (Fabini, 2015). If all the electricity in the United States were to be generated by PSCs using the most well-deliberated OIHP, the annual consumption of lead would be 160 tons (Fabini, 2015). Eliminating Pb from PSCs is the only long-term solution to the Pb-toxicity problem, even though PSCs may be managed and regulated to decrease environmental Pb discharge. The quantity of harmful components permitted in consumer or domestic niche applications, such as portable PVs, is extremely low (Hailegnaw et al., 2015). The band alignment between the perovskite material and the selective materials of n-type and p-type is crucial for effective charge extraction. In particular, the electron transport layer's conduction band edge should be lower than the perovskites, while the hole transport layer's valence band edge should be higher. This relationship is illustrated in Figure 2.

United States, Occupational Safety and Health Administration (OSHA), for instance, classifies lead and its compounds as very dangerous and has established a legally acceptable exposure limit of 0.05 mg/L for general industry (Levin et al., 1997). Due to the high expense of creating Pb-based PSCs and the need to invest heavily in protecting workers' health from the metal's narcosis and eye/nose/throat irritation. The necessity for organic positive ions to cover the "A-site" in the PVK assembly is another major issue with existing lead-based bulk OIHPs. These organic compounds have a mild interaction with the metal-halide octahedra at PSC circumstances when the inorganic cations are present (Brunetti et al., 2016).

Although PVKs include ammonia functional groups in their crystal structure, the organic species inside them are more hygroscopic, making them more susceptible to deterioration when exposed to air (Leijtens et al., 2015; Rong et al., 2015). Lead and chemical instability of PSCs based on lead-containing bulk OIHPs are the key difficulties. To solve these issues, researchers must identify novel PVK options that are innocuous and firm while

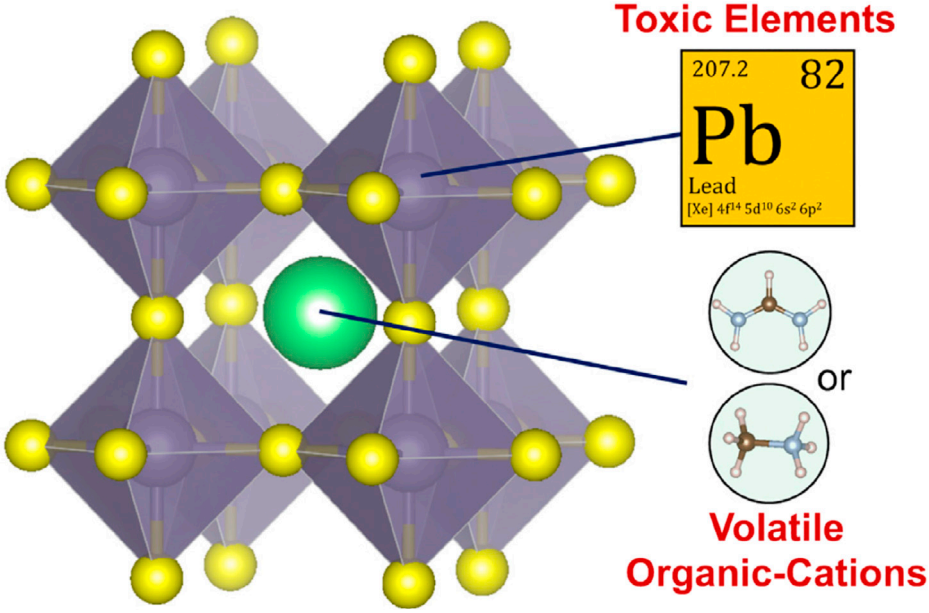


FIGURE 1
The lattice assembly of common OIHPs.

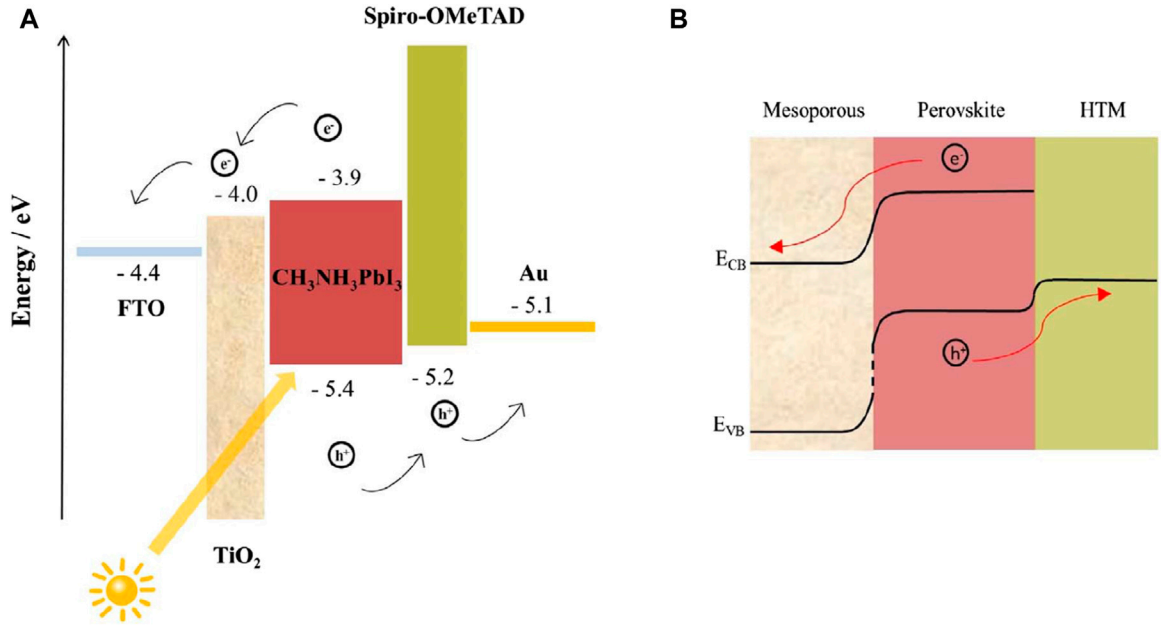


FIGURE 2
**(A)** A typical PSC energy diagram shows the energy levels of materials in different layers and **(B)** the band-bending of energy levels during charge separation.

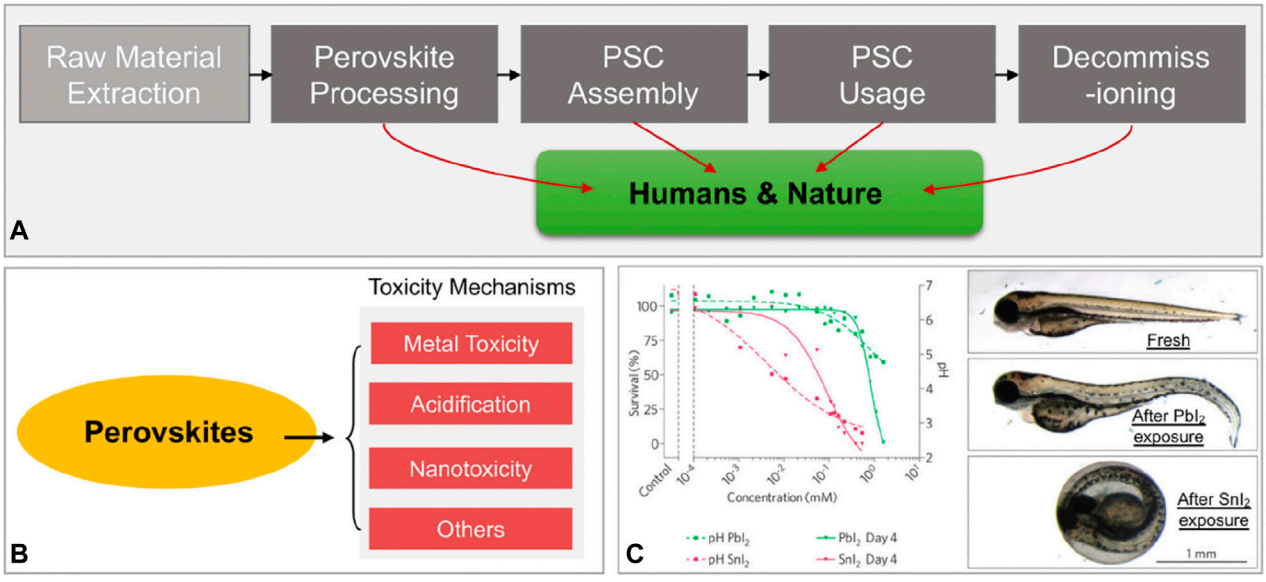


FIGURE 3
Toxicity evaluation and mechanisms in PVKs **(A)** PVK solar panels have an average projected lifetime altered (Babayigit et al., 2016). **(B)** Possible pathways of PVK toxicity, **(C)** Biological experiment outcomes utilized to evaluate Pb and Sn-based PVK toxicity (Jellicoe et al., 2016).

hitherto possessing sufficient PCE as an alternative to the currently employed lead-based PSCs. From this viewpoint, this paper primarily emphasizes the critical need to pinpoint the historical roots of the current PVK light-absorber materials' inherent toxicity and instability, and then address approaches to designing new environmentally friendly, stable PVKs. Future synthesis of novel lead-free PVK compounds is discussed to round up the paper.

## 2 Evaluation of prospective new PVKs' effects on the environment and their durability over time is essential

Getting the basic stuff out, synthesis/processing of cells, cell assembly, utilization, and decommissioning of cells are the usual stages in the life span of a PSC panel (Volans, 1987; Babayigit et al.,

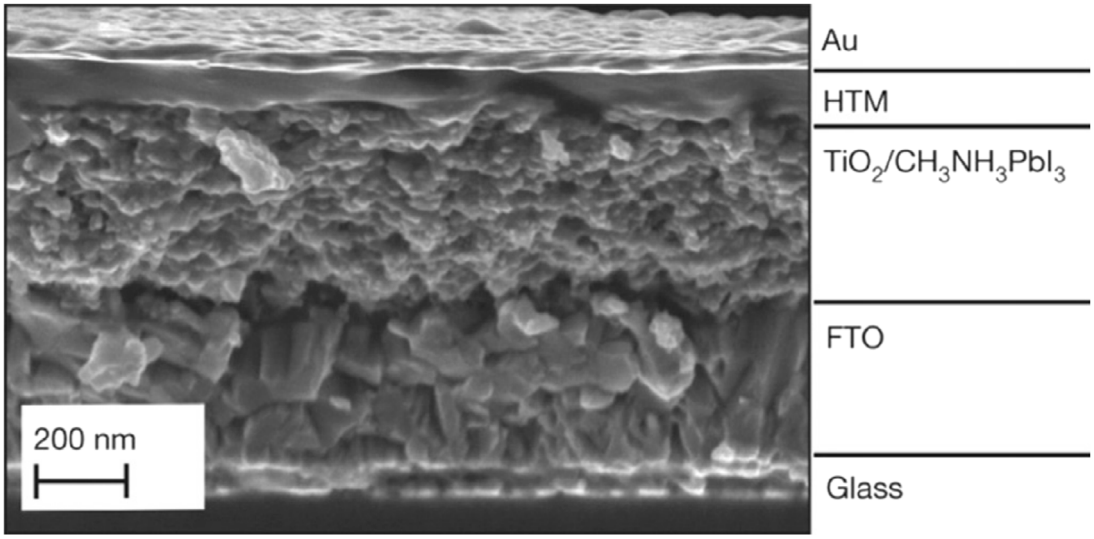


FIGURE 4
Perovskite solar cell cross-sectional SEM picture (Patrick et al., 2015).

2016), as illustrated in Figure 3A. Dangerous PVK-formed species will be released during all these phases, but it is too soon to do a full life cycle analysis of the PSC technology. Consequences like as land and water degradation are inevitable, as is the introduction of these toxins into the food chain, which ultimately reaches human people (Florence et al., 1988). Possible catastrophic incidents during PSC production, transit, storage, and use, such as fire or floods, provide additional environmental concerns (Dauvalter, 1955). As a result, Pb's indirect toxicity has far-reaching effects on human health and the natural world. In addition, PVKs may be detrimental to ecosystems and people through a variety of different processes, such as acidification and nanotoxicity (see Figure 3B).

Sn-based PSCs, for instance, have been shown to attain PCEs of 10%, making them a promising green option for PSCs. Recent research (Babayigit et al., 2016), however, shows that in Sn-based PVK materials, oxidation may proceed rapidly in ambient or aqueous settings, resulting in the creation of hydroiodic acid (Babayigit et al., 2016; Abate, 2017).

Zebrafish study shows that Strontium Iodide is more intensely lethal when compared to Lead Iodide (Figure 2C). The greater acidification effects of Sn2+ compared to lead ions are largely to blame for this. Nanoscale lead-based and lead-free PVKs for PSCs and optoelectronics are expected (Im et al., 2014; Jellicoe et al., 2016). Nanoscale materials harm cells and biological systems, so, probably, nanoscale PVK materials are also dangerous.

The utilization of a mesoporous layer in the mesoporous architecture facilitates the expeditious extraction of photoinduced electrons from the perovskite material. This results in a reduction of the electron transport distance and eliminates the need for a high level of crystal quality to achieve effective light absorption (Tétreault et al., 2010). Nevertheless, in comparison to other arrangements, mesoporous perovskite solar cells often exhibit a reduced $V_{oc}$ (Kang et al., 2016) and diminished light absorption beyond 720 nm wavelengths (Chen M. et al., 2016). The need for a perovskite overlayer to avoid mesoporous layer-HTL contact might cause short circuits (Yan et al., 2016). Moreover, there is an ongoing dispute over the role of the mesoporous layer, especially considering the remarkable efficiencies demonstrated by two-dimensional perovskite solar cell (PSC) devices. The highest recorded efficiency, as reported in reference (Fu et al., 2014), is at 20.7%. Titanium dioxide ($TiO_2$) is used as a mesoporous layer due to its broadband gap energy of 3.5 eV, chemical and thermal stability, photodegradation resistance, non-toxicity, and cost-effectiveness (Haruyama et al., 2015; Sabba et al., 2015). Figure 4 shows that mesoporous layer thickness affects perovskite polycrystal penetration into $TiO_2$ pores.

In a study conducted by authors (Wang et al., 2016), it was observed that a mesoporous layer of $TiO_2$ with a thickness ranging from 260 nm to 440 nm adequately filled the pores of mesoporous $TiO_2$, as depicted in Figure 5. These results suggest that between these bounds lies the sweet spot for maximizing light absorption while minimizing recombination due to route length. When testing the solar efficiency of each component, it was discovered that the mesoporous $TiO_2$ device, although thinner, performed well Figure 6. One possible explanation is that the higher electron density in $TiO_2$ improves charge transfer and collecting efficiency (Wu et al., 2017).

Nanoscale PVKs may be harmful due to their fibrous structure (Xiao Z. et al., 2015; Ju et al., 2017a; Ju et al., 2018), and radical species group (Ming et al., 2016). A meaningful evaluation of the toxicity of PVK compounds, both those already in use and those that have yet to be discovered, necessitates the prompt construction and implementation of a systematic system of biological investigations. Despite the potential importance of this avenue for PSC research, nothing has been done thus far.

Figure 7 shows that water, light, heat, and oxygen are the most detrimental to the stability of a PVK material. A wide range of processes, including polymorphic transformation, hydration, ion transport (Ke et al., 2017a), breakdown, and oxidation, are

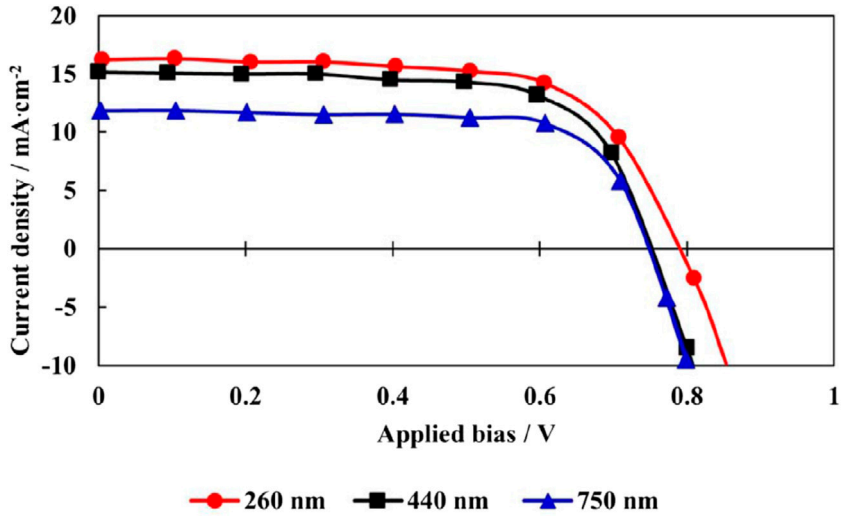


FIGURE 5
Estimating the IV curves of a device, coating thickness, and pore filling in a perovskite (Wang et al., 2016).

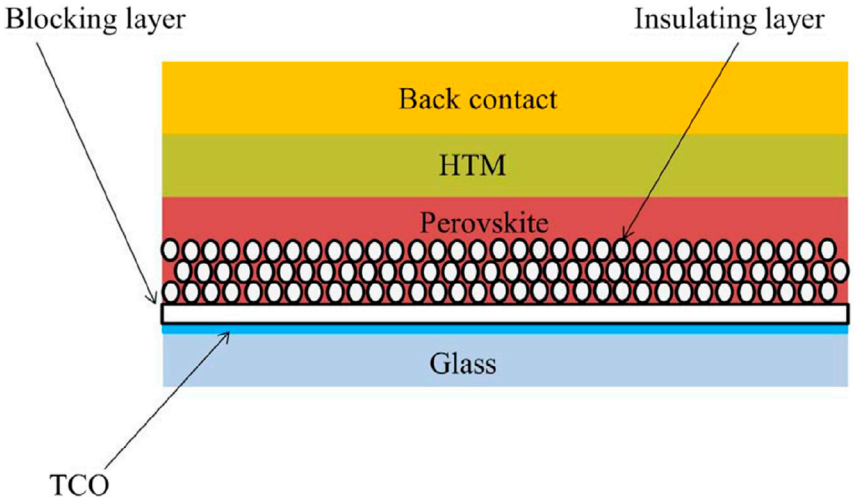


FIGURE 6
Mesoporous insulating-oxide-based PSC (Chung et al., 2012).

responsible for the degradation of OIHPs by these agents. While Pb-based OIHP deterioration has been extensively investigated in recent years, our knowledge of Pb-free PVKs is still in its infancy. The stability problem of upcoming PVK materials may be much more complicated than that of Pb-based OIHPs, according to certain studies in the literature.

Many decay pathways may be active simultaneously. $CsSnI_3$, a lead-free candidate PVK material with a 1.3 eV optical bandgap and decent carrier mobility, is one such example (Yin et al., 2017). CsSnI3 PVK is thermally stable because of its inorganic composition and robust covalent bonding for its lattice assembly (Volonakis et al., 2017). The "black" phase of g-$CsSnI_3$ rapidly undergoes a "yellow" polymorph transformation when exposed to air (Saparov et al., 2015; Slavney et al., 2016). Nevertheless, oxygen may quickly oxidize Sn (II) in $CsSnI^3$ to Sn (IV), turning it into $Cs_2SnI_6$ (Giustino and Snaith, 2016).

Moisture from the air may also penetrate $CsSnI_3$ PVK thin films, where it can form hydrates and break down the material into metal halides. The PCE of PSCs based on CsSnI3 may drop precipitously due to a combination of these degrading processes. Due to their extreme instability in the ambient environment, they can decay in a matter of minutes if not enclosed.

It is difficult to examine these pathways in isolation, but doing so is essential if we are to solve the PSC instability problem once and for all. In addition, there are several other Pb-free PVK possibilities whose stability and deterioration have been poorly researched (Xiao et al., 2017a; Xiao et al., 2017b; Yang et al., 2017), including $CsGeI_3$, CsSnxGe1-x$I_3$, Cs2Ti$I_6$-xBrx, and $Cs_2AgBiBrI_6$. Research into their resistance to the major environmental variables (humidity, light, heat, oxygen) and possible breakdown mechanisms is promising. New, Pb-free, stable PVKs for PSCs can be designed using the

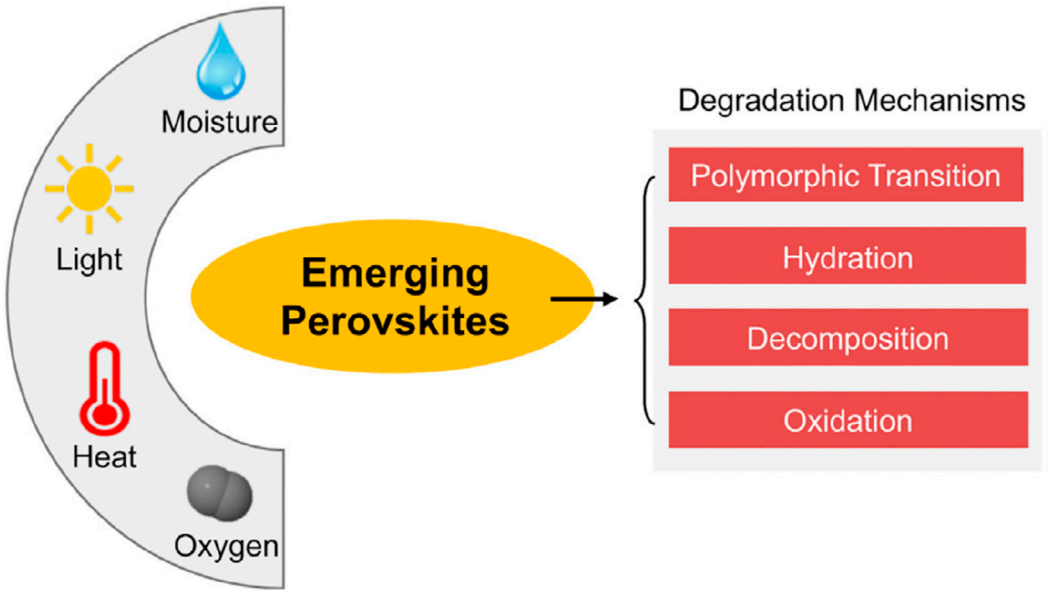


FIGURE 7
Degradation of new PVK materials due to environmental variables and their processes.

information gleaned by studying the stability of these developing PVKs.

## 3 Theory and experiment required to find nontoxic, stable PVKs for PVs

Theoretical simulations screen the enormous number of PVK family compounds and derivatives to find safe and stable candidate PVKs. There are typically two phases to such materials screening processes. Finding potential elements to substitute for Pb in current Pb-based OIHPs is the first step in solving the toxicity problem. Substitutes for PVKs in PV applications must have many of the same fundamental electrical, conveyance, and ocular features. Group IV elements $Sn_{2+}$ and $Ge^{2+}$ are often cited in the literature as suitable lead ion substitutes. Lead-free Sn- and germanium-based PVKs for PV applications have emerged from this logic. Sn-based PSCs have PCE approaching 10% (Ju et al., 2017b), even though Sn2+ may be quickly oxidized to $Sn^{4+}$, lowering performance. Potential Pb-free PVK candidates can also be identified using an electrical structure-based approach.

Pb-based OIHPs have high PCEs because the Pb lone-pair 6s orbital has a strong antibonding interaction with the I 5p orbital, allowing for longer carrier lifetimes and diffusion lengths (Zhang et al., 2017). Several researchers have focused on PVKs made from non-traditional metals because of the presence of lone-pair ns2 (McMeekin et al., 2016; Nakajima and Sawada, 2017; Ali et al., 2018a). New compounds having antibonding contact between orbitals around the valence band maximum can likewise exhibit band-edge behaviour like lead-based PVKs. Skutterudite structure has been proposed, for instance (Dai et al., 2017). Unlike lead-based PVKs, $IrSb_3$ possesses a band-edge feature indicative of p-p* antibonding interaction. The crystal structure for PVK materials provides another angle from which to hunt for promising Pb-free PVK options.

Replace Pb2+ with an aliovalent metal cation and the resulting PVK structure will have a different chemical formula from the usual AB(II/III/V) X3/X6/X9 (Zhao et al., 2017a; Zhao et al., 2017b). The electrical structure of the compounds will be altered because of this structural alteration (Sakai et al., 2017). Figure 8A shows how crystal structure and chemical composition can be used to create novel PVK-type compounds with favourable electrical structures for PV applications.

To accurately anticipate the stability of PVKs, a theory-experiment integrated method is required because of the complexity of the problem (Pang et al., 2016; Sun and Yin, 2017) To get a general idea of the stability of the PVK phase, a common empirical rule is to utilize Goldchmidt's tolerance factor (t). Cubic assemblies are suggested by fits in the 0.9% t% one range for PVKs, whereas orthorhombic assemblies are suggested by fits in the 0.71%–0.9% t% one range. Other configurations include the hexagonal assembly, for t% 0.71 or t R 1. Figure 8B displays a flow chart for showing non-hazardous metal-based PVK intrants with PV constancy. This technique logically combines theory and experiment. Figure 8A depicts the first step of the process, which involves identifying a suitable metal-free PVK that does not include lead. Although the organic A-site positive ion is intrinsically unstable, positive ions such as caesium ions (Castelli et al., 2012; Korbel et al., 2016) are employed as replacements (Schmidt et al., 2017; Takahashi et al., 2018) due to their sturdier ionic interaction through unknown negative ions.

The most promising PVK candidates may be identified by combining A with B-site replacement. This method has been used to effectively anticipate and synthesise compounds like $CsSnI_3$, $Cs_2AgBiBr_6$, and $Cs_2TiBr_6$, although there may be additional PVK options that are less toxic and more stable (Lee et al., 2012; Burschka et al., 2013; Pilania et al., 2016; Li Z. et al., 2018). Several alternatives to B-site ions in PVK structures, including monovalent metals and trivalent metals (Xiao et al.,

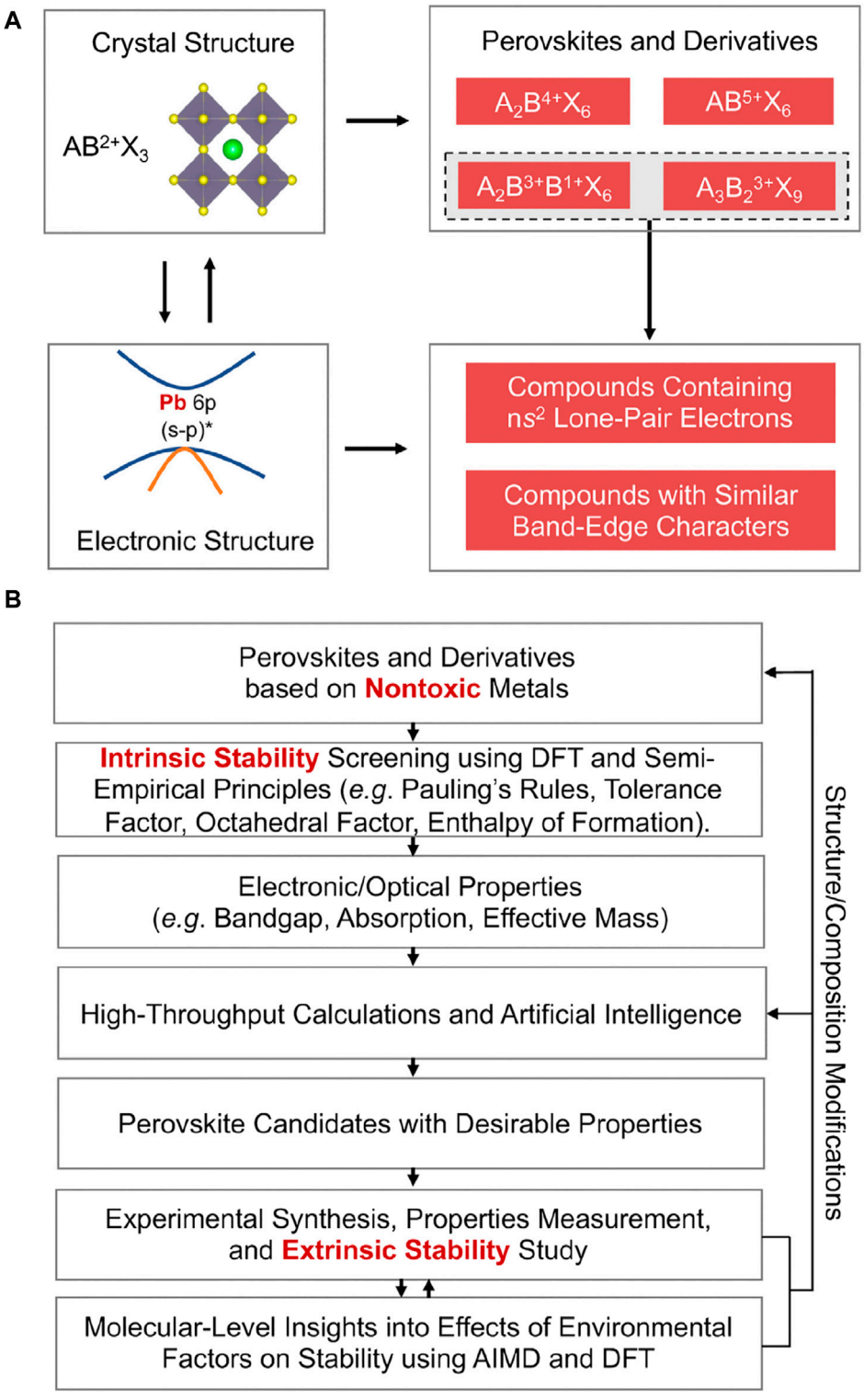


FIGURE 8
Strategies for Finding Stable, Nontoxic PVKs **(A)** Example of the use of crystal structure and electrical structure information to potentially choose stable, non-toxic PVK candidates for PSCs. **(B)** A schematic showing how to find safe, stable PVK candidates to use in PSCs (Debbichi et al., 2018).

2014; Chen et al., 2018a; Ávila et al., 2017; Xiao J. et al., 2015; Elumalai et al., 2016), have been proposed. Substituting a tetravalence metal for the B-site ion stabilizes vacancy-order double PVKs (Kalyanasundaram and Grätzel, 1998; Leijtens et al., 2013). The same atoms in various valence states can substitute the B-site ion in electronic double PVKs (Xin et al., 2011).

Using Figure 8B's manufacturing cycle, first, validate new compounds' intrinsic or thermodynamic stabilities using "density

functional theory (DFT)" based design to guarantee they have the requisite PV-related electronic/optical properties. As shown in Figure 3, when the PVKs have been synthesized, they are put through a series of experiments to determine how stable or degradable they are in the presence of various external environmental stimuli.

DFT-based mechanistic research complements experimental studies (Bi et al., 2013; Leijtens et al., 2014). These parallel theory-experiment studies (Son et al., 2014; Zuo et al., 2015) show how to modify PVK crystal structure/composition to find more stable PVK candidates. As can be seen in Figure 4B, the entire stability-screening procedure considers the crucial electrical assembly and the PVKs' photovoltaic properties.

High amount simulated ingredients strategy can anticipate lead-free PVK ingredients for PV utilizing computational quantum-mechanical, thermodynamic, database development, and intelligent data-mining methods. Although useful, these calculations cannot replace a full material simulation, and they often only solve a portion of the design issue. The DFT-computed descriptors are useful for screening candidate materials and determining their important features (Agresti et al., 2016).

Pauling's principles (Ball et al., 2013), are computational descriptors for intrinsic stability. Bandgap and effective mass can approximate light absorption and carrier mobility. The basic components of a material can provide an approximation of its cheap cost and nontoxicity. Descriptors screen candidates with a PVK structure and its modifications for materials with the right attributes (Ball et al., 2013).

High-throughput computational design is computationally expensive due to the huge conformation space and the enormous number of acceptable descriptors for essential properties, many of which are derived by more precise functional modelling (Wojciechowski et al., 2014). In divergence, a good machine learning model may be taught using existing data or data derived through computations. To find novel candidate materials with desirable qualities, this approach may be applied to the periodic table, yielding insights, and guiding experimental design (Niu et al., 2015). PVK stability and bandgap have been estimated in previous works using a variety of techniques based on the identification of pertinent properties (Christians et al., 2014; Qin et al., 2014; Jeon et al., 2015).

# 4 Advances in lead-free perovskites

## 4.1 Tin perovskites

Group 14 components Tin's 5s2 electrical configuration resembles lead's 6s2. With a similar outer electron shell structure to lead (Pb) but a smaller ionic radius, tin may be a preferable option (Zhang Q. et al., 2018). Tin can replace lead in PSCs (Wang X. et al., 2019). Tin is cheap, non-toxic, and electrically comparable to lead (Shanon, 1976; Ke et al., 2017b). The most researched lead-free perovskite alternative is tin-based (Fu, 2019). Tin halide-based perovskites have low exciton binding energy, a tiny band gap, and excellent carrier mobility (Liu X. et al., 2020). Sn-based perovskites offer several advantages for solar cells, but their unstable divalent Sn states make them extremely conductive and inefficient (Song et al., 2017). Tin-based lead-free PSCs are ineffective because $FASnI_3$ perovskites rapidly crystallise and oxidise, resulting in rough morphology and large defect concentrations (Liu X. et al., 2020). Table 1 lists current tin-based perovskites and ways to improve them.

## 4.2 Perovskites with a composition based on bismuth

The electrical configuration of group 15 element bismuth is $Bi^{3+}$ (6s2). Bismuth is less toxic than lead and has many dimensions due to its $BiX_6$3 octahedron structure (Shanon, 1976; Zhang et al., 2023). Subsalicylate and bismuth subcitrate are therapeutic (Ganose et al., 2017). Chronic bismuth use can induce encephalopathy and renal failure (Ganose et al., 2017). Bismuth perovskites are attractive because of their lead-like isoelectronic valence shell (Lozhkina et al., 2018). Like lead (1.21 A°), $Bi^{3+}$ is stable and has an ionic radius of 1.05 A° (Wani et al., 2015; Liu et al., 2022). Bismuth-based perovskites can replace lead-based ones due to their optoelectronic properties, environmental friendliness, and light, heat, and moisture resistance (Dai and Tüysüz, 2019). Bismuth-based perovskites have the most stable optical and structural characteristics since optical parameters did not change after 3 months without surface passivation (Kim et al., 2016).

Table 2 lists bismuth-based perovskites and strategies for overcoming obstacles.

## 4.3 Perovskites with a composition based on Sb (antimony)

Group 15 element antimony (Sb3+) has an ionic radius of 0.75 A° and an electronic configuration of 5s2 (Wang X. et al., 2019). An alternative to lead, antimony is non-toxic and twice as affordable as Sn per kilogram (Lozhkina et al., 2018). Irina Shtangeeva et al. found that high amounts of antimony in growth media were very hazardous to plants, resulting in a significant decrease in leaf and root biomass output (Liu Y. et al., 2019). The alignment of Sb's 5s and 5p orbitals with p-block anions makes it a lone pair effect heavy hitter, and there are several advantages to being in the 3+ oxidation state (Lozhkina et al., 2018).

Trivalent Sb, which has one set of 5s2 electrons instead of lead, is an option. Therapeutics are the primary use of antimony compounds (Lozhkina et al., 2018). Liu et al. (2018) performed a theoretical evaluation of $Cs_3Sb_2X_9$'s optoelectronic characteristics. The computed carrier mobilities of $Cs_3Sb_2I_9$ indicate an appropriate band energy gap for hydrogen production and CO2 reduction due to enhanced electronic mobilities. $Cs_3Sb_2I_9$'s photocatalytic activity is enhanced by the significant difference in hole and electron mobilities, which slows electron-hole recombination. The photovoltaic performance of $Cs_3Sb_2I_9$ is superior to lead-based perovskites, making it a viable replacement (Singh et al., 2018). To manufacture solar cells efficiently, issues with antimony-based perovskites must be resolved. In terms of solar performance, solution-processed Sb-based perovskites are best suited for the dimer phase (Karuppuswamy et al., 2018). The amorphousness and pinholes in the surface form of the zero-dimensional dimer

TABLE 1 Current tin-based perovskites and their fabrication methods.

| Name of the compound | Electrical properties (Voc (V), Jsc (mA $cm^2$) | Fabrication methods | Reference number |
|---|---|---|---|
| $CsSnI_3$ | 0.3816, 25.71 | One-step/Weak hydrazine atmosphere | Shum et al. (2010), Chung et al. (2012), Kumar et al. (2014), Marshall et al. (2015), Chen et al. (2016b), Marshall et al. (2016), Moghe et al. (2016), Song et al. (2017), Wang et al. (2020), Ban et al. (2021) |
| $CsSnBr_3$ | 0.86, 22.13 | Easy solvothermal procedure | Chen et al. (2016b), Gupta et al. (2016), Li et al. (2018b), Coduri et al. (2019), Bonomi et al. (2020), Fang et al. (2021) |
| $CsSnCl_3$ | 0.87, 19.82 | Easy solvothermal procedure | Chen et al. (2016b) |
| $Cs_2SnI_6$ | 0.53, 5.48 | Vapour deposition, solid-state reaction, thermal evaporation, and rapid annealing | Qiu et al. (2017), Umedov et al. (2020) |
| $MASnI_3$ | 0.88, 16.8 | Spin coating, Thermal evaporation | Qiu et al. (2017) |
| $FASnI_3$ | 22.5, 58 | Antisolvent dripping + single-step spin-coating | Koh et al. (2015), Liao et al. (2016), Shi et al. (2017a), Shao et al. (2017), Meng et al. (2020a) |
| $FASnI_2Br$ | 6.82, 54.5 | Spin coating + Annealing + Thermal evaporation | Zhang et al. (2016a) |

TABLE 2 Current bismuth-based perovskites and their fabrication methods.

| Name of the compound | Electrical properties (Voc (V), Jsc (mA $cm^2$) | Fabrication methods | Reference number |
|---|---|---|---|
| Methylammonium iodo bismuthate ((CH3NH3)3Bi2I9) | 0.51, 0.7 | Single-step spin coating/low-temperature solution technique | Kulkarni et al. (2017) |
| $Cs_3Bi_2I_9$ | 0.84, 22.13 | Easy solvothermal procedure | Sanders et al. (2018) |
| $AgBi_2I_7$ | 0.57, 3.31 | Synthesis focused on finding solutions | Singh et al. (2016) |
| $MA_3Bi_2I_9$ | 0.58, 0.45 | Coating with spin, annealing, and sintering | Shtangeeva et al. (2011a), Zhang et al. (2016b) |

TABLE 3 Current antimony-based perovskites and their fabrication methods.

| Name of the compound | Electrical properties (Voc (V), Jsc (mA $cm^2$) | Fabrication methods | Reference number |
|---|---|---|---|
| $Cs_3Sb_2I_9$ | 0.76, 2.83 | Approach to solution processing | Karuppuswamy et al. (2018) |
| $(NH_4)_3Sb_2I_9$ | 1.04, 1.16 | An approach to crystallization that does not involve solvent vapour | Weber et al. (2019) |
| $(CH_3NH_3)_3Sb_2I_9$ | 0.63, 5.10 | Coating using spin, followed by annealing and sequential depositing | Zuo and Ding (2017) |
| $Rb_3Sb_2I_9$ | 0.56, 4.26 | Method for vapour diffusion crystallization | Chen et al. (2019), Yang et al. (2021) |

of methylammonium antimony iodide cause its poor PCE (Zuo and Ding, 2017). Table 3 lists antimony-based perovskites and strategies for overcoming obstacles.

## 4.4 Perovskites with a composition based on germanium

The ionic radius of $Ge^{2+}$ is 0.73 Å, and its electronic configuration is 4s2 (Wang X. et al., 2019; Yang et al., 2021). It is a group of 14 elements. Germanium is easy to find in nature, and its pure organogermanium products are safe (Schauss, 1991; Ganose et al., 2017). Germanium has little toxicity, except for tetrahydride germane (Gerber and Léonard, 1997). The covalent character and higher electronegativity of Germanium make it a possible alternative to lead PSCs (Kopacic et al., 2018). Ping-Ping Sun et al. found that $MAGeI_3$ is theoretically very comparable to $MAPbI_3$ in terms of band gap, stability, outstanding optical properties, and hole and electron conductivity (Sun et al., 2016). The stability and effectiveness of Ge and Sn as lead mono substitution options have been demonstrated in lead-free perovskite studies (Ali et al., 2018b). It is thought that perovskites based on Ge, as opposed to tin

TABLE 4 Current germanium-based perovskites and their fabrication methods.

| Name of the compound | Electrical properties (Voc (V), Jsc (mA $cm^2$) | Fabrication methods | Reference number |
|---|---|---|---|
| $CsSn0.5Ge0.5I_3$ | 0.074, 5.7 | Solid-state reaction | Chen et al. (2019), Li et al. (2019), Meng et al. (2019) |
| $MAGeI_3$ | 0.15, 4.0 | Spin coating + Annealing + Sequential deposition | Krishnamoorthy et al. (2015) |
| $MAGeI_{2.7}Br_{0.3}$ | 0.68, 0.460 | Combination of sonication, spin coating, and thermal evaporation | Krishnamoorthy et al. (2015) |

or lead, have smaller bandgaps due to the higher orbital energy of Ge (4s) as compared to Sn (5s) and Pb (6s). Perovskites based on Ge, on the other hand, exhibit larger bandgaps compared to those based on tin and lead. The fact that the [$GeI_6$] octahedral structure is structurally deformed is the primary cause of the unexpected finding (Liu et al., 2018). Germanium compounds may block mutagenic activity and prevent cancer formation under certain conditions, demonstrating they are neither carcinogenic nor mutagenic (Gerber and Léonard, 1997). The tumour incidence was reduced in rats that were administered 5 parts per million of sodium germanate in their drinking water during their lives (Gerber and Léonard, 1997).

While germanium perovskite has several benefits, it has some problems that must be addressed for increased efficiency. Commercial usage of germanium-based perovskites in photovoltaics has been hindered by poor performance (below 0.2%) and device instability (Kopacic et al., 2018). In germanium-based PSCs, $Ge^{2+}$ oxidation is the main issue. In PSCs based on germanium, this results in poor performance (Wang X. et al., 2019). On the other hand, if future research can reach efficiencies beyond 10%, mixed Ge/Sn-based perovskites might be a promising material. The exorbitant price of Ge is one potential drawback of solar cells based on Ge (Ke and Kanatzidis, 2019). Table 4 lists antimony-based perovskites and strategies for overcoming obstacles.

## 4.5 Perovskites with a composition based on titanium

Titanium (IV), a non-toxic element, is abundant on Earth and has exceptional stability (Ju et al., 2018). $Ti^{4+}$ has an electronic structure of 3p6 and an ionic radius of 0.53 Å (Wang X. et al., 2019). Common reasons for gridlock in Pb-free perovskites include instability, undesirable defect states, and insufficient band gaps (Bansode et al., 2015). Table 5 displays the titanium-based perovskites that are currently used.

## 4.6 Perovskites with a composition based on copper

Non-toxic copper is abundant and has good charge mobility (Sani et al., 2018). $Cu^{2+}$ has an ionic radius of 0.73 Å and an electronic configuration of 3d9 (Ke et al., 2017b; Wang X. et al., 2019). The transition metal copper is stable. In aerobic environments, $Cu^{2+}$ can form stable compounds with a high visible absorption coefficient (Cortecchia et al., 2016). While copper's ($Cu^{2+}$) stable oxidation state makes it a viable alternative to lead, the halide octahedron's corner-sharing network is constrained by its smaller ionic radius. There are a lot of effective hole masses, a low intrinsic conductivity, and a low absorption coefficient in the perovskite layer (Okano and Suzuki, 2017). Perovskites made of copper that have been used so far are listed in Table 6.

## 4.7 Bimetallic or double perovskites

Substituting another B′ cation for half of the B site cation in the general formula of the perovskite structure ABO3 results in $A_2B_2O_6$ or $A_2BB'O_6$, two forms of double perovskites (Saha-Dasgupta, 2020). Due to the nanocrystal surface energy in metastable phases, nanoscale, double perovskite materials that were limited to single monolayers exhibited quantum size effects and enhanced stability. Stable nanocrystals include $Cs_2AgBiI_6$, which cannot be mass-produced. The combinatorial compositions and quaternary nature of double perovskite materials provide them with electronic structure engineering flexibility and bandgap tunability (Karuppuswamy et al., 2018; Khalfin and Bekenstein, 2019). Double perovskites made of lead are more environmentally friendly than other lead-free structures, and they have great chemical stability, electronic dimensions, and substitutional chemistry. LEDs, X-ray detectors, photocatalytic dye sensors, solar cells, and lead-free double perovskites are only a few examples of the many renewable energy and optoelectronic applications for these materials (Dave et al., 2020; Ghrib et al., 2021; Grandhi et al., 2021). Recent lead-free perovskites $Cs_2SbAgCl_6$, $Cs_2InAgCl$, $Cs_2BiAgCl_6$, and $Cs_2BiAgBr_6$ exhibit outstanding optoelectronic properties because of their low carrier effective masses and detectable bandgaps (Volonakis and Giustino, 2018). You may see a selection of the double perovskites that have been utilized thus far in Table 7.

## 4.8 Perovskite oxide without lead

$BiMnO_3$ is the sole transitional-metal perovskite oxide with unique properties including insulating and high ferromagnetism in bulk. According to a 2015 study by Di'eguez et al., solar applications might be possible using BiMnO3 films that have lower band gaps compared to ferroelectric oxides (Diéguez and Íñiguez, 2015).

TABLE 5 Current titanium-based perovskites and their fabrication methods.

| Name of the compound | Electrical properties (Voc (V), Jsc (mA $cm^2$) | Fabrication methods | Reference number |
|---|---|---|---|
| $Cs_2TiBr_6$ | 0.88, 3.84 | A two-stage process for vapor deposition | Chen et al. (2018b) |
| $Cs_2TiI_2Br_4$ | 0.87, 3.80 | A two-stage process for vapor deposition | Liu et al. (2020b) |
| $Rb_2TiBr_6$ | 0.91, 3.91 | A two-stage process for vapor deposition | Liu et al. (2021) |
| Hybrid Ti-based PSCs | 1.02, 3.98 | A two-stage process for vapor deposition | Ju et al. (2018) |

TABLE 6 Current copper-based perovskites and their fabrication methods.

| Name of the compound | Electrical properties (Voc (V), Jsc (mA $cm^2$) | Fabrication methods | Reference number |
|---|---|---|---|
| $MA_2CuCl_{0.5}Br_{3.5}$ | 0.290, 0.021 | Two-step vapour deposition method | Cortecchia et al. (2016) |
| $(CH_3(CH_2)_3NH3)2–CuBr_4$ | 0.88, 1.78 | Two-step vapour deposition method | Cui et al. (2015) |
| $MA_2CuCl_2Br_2$ | 0.256, 0.216 | Sintering + Spin coating | Cortecchia et al. (2016) |

TABLE 7 Current bimetallic or double perovskites and their fabrication methods.

| Name of the compound | Electrical properties (Voc (V), Jsc (mA $cm^2$) | Fabrication methods | Reference number |
|---|---|---|---|
| $Cs_2AgBiBr_6$ | 1.04, 1.78 | Annealed at 250° | Wu et al. (2018) |
| $Cs_2NaBiI_6$ | 0.48, 1.97 | Hydrothermal process with a single step | Zhang et al. (2018b) |

Researchers Yuji Okamoto et al. demonstrated that dye-sensitized solar cells using perovskite oxides ($SrTiO_3$, $CaTiO_3$, and $BaTiO_3$) could achieve a high Voc in cells that were phase-pure (Okamoto and Suzuki, 2014).

# 5 Possible methods for enhancing performance in lead-free perovskites

Using additives and adjustments to the solar cell fabrication process, lead-free PSCs may be made more efficient and stable. One or more of the following goals can be accomplished with the introduction of additives: control of oxidation, reduction of vacancies, alteration of the optical bandgap, increase of the fill factor (FF), or improvement of efficiency. The utilisation of appropriate techniques in fabrication can successfully address issues such as inadequate crystallisation, unfavourable morphology, and undesirable defects. This is crucial in achieving uniform and defect-free perovskite films without any pinholes (Ke et al., 2017c).

## 5.1 Tin, bismuth, Sb, and Ge-based perovskites additives overcome obstacles

Data from (Ke et al., 2017c; Meng et al., 2019) suggests that additives play a crucial role in lead-free perovskites. Few research has examined the impact of additives on optical bandgap. The power conversion efficiency (PCE) grows when the optical bandgap narrows, as demonstrated in (Ke et al., 2017c; Meng et al., 2019). Tin-based perovskites had increased efficiency with additives, whereas Bismuth and antimony-based ones had lesser efficiency. This may be because Bismuth and antimony-based perovskites have greater optical bandgaps than tin-based ones. To increase PCE in bismuth and antimony-based perovskites, chemicals that lower the optical bandgap can be utilised. When additives raise the optical bandgap of tin-based perovskites, the PCE may decrease. In experiments (Ke et al., 2017c) adding ethylenediammonium (ED) enhanced optical bandgaps by 1.45 eV, 1.53 eV, and 1.92 eV at 0%, 10%, and 25% concentrations. PCE decreased with loading of 0, 8, and 23%, resulting in 1.42%, 6.98%, and 2.45%, respectively. This is because 28% loading results in a greater optical bandgap (Ke et al., 2017c). Optimising additive amounts leads to improved efficiency by maintaining or narrowing the optical bandgaps. Results in (Meng et al., 2019) found that adding poly (vinyl alcohol) PVA did not change the predicted optical bandgap of $FASnI_3$ at 1.39 eV. The high PCE of 8.96% might be attributed to the PVA molecule being near the grain boundary of the perovskite layer. Optimising the selection and number of additives in perovskite compound production is crucial for producing highly efficient lead-free solar cells. Table 8 shows the various effects of adding additives to the above perovskites.

# 6 Recent breakthroughs/future perspectives in PSC

Recent advancements in the field of PSCs have focused on using different treatments, introducing hole transport materials, and including chiral compounds to enhance their efficiency and open-circuit voltage (Voc). These strategies will be further explored in the following discussion.

TABLE 8 Challenges tackled by adding additives.

| Recent perovskites used | Additives used | Effect of adding additive | Challenges tackled by employing effective fabrication | Reference number |
|---|---|---|---|---|
| Tin | Butylammonium iodide | Changed the orientation of crystal growth and enhanced grain-to-grain contact | Sequential deposition | Shtangeeva et al. (2011b) |
| | Ethylene diammonium di iodide ($EDAI_2$) | The first device's performance reached a peak of 7.5% and subsequently improved to a high of 9.01% | Pulsed laser deposition (PLD) technique | Jokar et al. (2018) |
| | $SnBr_2$ | This addition has proven to be effective by enhancing the PCE to 4.5% and exhibiting stability of 100 h | Anti-solvent dripping | Heo et al. (2018) |
| | $SnCl_2$ | The specific energy output (Jsc) of the solar cell was 15.0 mA/cm2, and the open-circuit voltage (Voc) was 385 mV; the PCE was 3.3% | Solution process | Tsai et al. (2017) |
| | $SnI_2$ | The solar cells' efficiency increased twofold, from around 0.78% to around 1.8%. There has been a reported rise of about 35% in the values of Jsc and Voc | Melt synthesis | Handa et al. (2017) |
| | $SnF_2$ | The outcome was a bandgap of 1.28 eV and a significant enhancement in the luminescence lifespan, surpassing the previous performance of the device by more than one magnitude | Annealing | Greul et al. (2017) |
| | Piperazine | Enhanced film coverage and reduced conduction of CsSnI3 films have been observed | Manufacturing in hydrazine-reducing vapour | Gu et al. (2018) |
| | Ammonium hypophosphite | Better Voc and device performance, together with higher stability, lower defect density, and enhanced film quality | Method of multichannel interdiffusion | Meng et al. (2020b) |
| Bismuth | N-methyl pyrrolidine (NMP) | Adding varying concentrations of NMP to the precursor solution changed the crystallization rate. Achieved a 60% improvement in Jsc and an efficiency boost of up to 0.33 per cent | Dissolution-recrystallization method | Kulkarni et al. (2017), Bai et al. (2018) |
| | 20% $BiI_3$ | Increasing the concentration of BiI3 causes a dramatic increase in the photocurrent density. With an additional 24% BiI3, 0.46 V Voc, and 0.63 mA Jsc, the PCE in Cs3Bi2I9 was found to be 0.25% | Method for fabricating films using two-step evaporation and spin coating | Ran et al. (2017), Ghosh et al. (2018) |
| Sb (ANTIMONY) | Methylammonium chloride | Demonstrated a PCE over 2% | Sequential reaction annealing | Jiang et al. (2018), Karuppuswamy et al. (2018) |
| | Toluene | Uniform film with 0.5% efficiency | Two-step deposition approach, Anti-solvent treatment | Hebig et al. (2016), Wang et al. (2019b) |
| Germanium | $CsGeX_3$ | Had 4.94% efficiency | Calibration of optical characteristics of lead-free inorganic PSCs is possible without annealing | Wang et al. (2019b) |

## 6.1 Using various hole transfer materials (HTM)

The data presented here emphasize the role that hole transport materials (HTMs) play in perovskite solar cell systems' ability to increase efficiency and Voc. Using poly (3-hexylthiophene-2,5-diyl) (P3HT) as the hydrogen transfer material (HTM), Sagar. M. Jain et al. (2019) found that the fabrication efficiency of (CH3NH3) 3Bi2I9 films was raised by 1.62%. When compared to the 1.12% efficiency attained with the conventional Spiro-OMeTAD HTL, this value is significantly greater. Min-Cherl Jung et al. (2015) used spiro-OMeTAD, C60, and P3HT, among other HTMs, to create MASnBr3 perovskite solar cell devices. In that order, the efficiencies were 0.002%, 0.221 per cent, and 0.35%. This shows that the efficiency of the solar cell devices was greatly affected by the HTM option, with P3HT showing the best efficiency out of the three HTMs that were evaluated. In addition, the lack of photocurrent and fill factor (FF) caused by spiro-OMeTAD's high resistance is the reason for its poor efficiency. Different HTMs can cause changes in the open-circuit voltage of the solar cell devices; this is supported by the fact that devices, including C60, achieve a higher Voc than P3HT devices. Overall, these findings underscore the critical role of HTMs in achieving improved efficiency and Voc in PSC devices and highlight the potential for P3HT as an effective HTM in this context.

## 6.2 Antisolvent therapy

A study conducted by Jiewei Liu et al. discovered that using a hot Ph-Cl antisolvent treatment prevented the electric shunting of the Solar System and an increase in the number density of nucleation sites in the film. When the film was annealed in an atmosphere with a low concentration of dimethyl sulfoxide (DMSO) vapour, the average size of the crystal particles increased. Furthermore, according to the reference, adding DMSO vapour during annealing increased the film quality (Song et al., 2018).

In 2017, Priyadharsini Karuppuswamy and colleagues produced films of $(CH_3NH_3)_3Sb_2I_9$ using antimony. They improved the film's surface morphology and device performance by employing Hydroiodic acid (HI) as an additive and treating it with Chlorobenzene (CB) Antisolvent Treatment. The alignment of the energy levels was also improved. As can be observed from the UV absorbance spectra, the increased surface coverage brought about by the combination of HI and CB treatment led to a higher absorption intensity (Karuppuswamy et al., 2018).

## 6.3 Interfacing manufacturing

After adding a hydrophobic scaffold to $(CH_3NH_3)_3Sb_2I_9$ films, several improvements were noticed. Grain size, crystallinity, crystallisation orientation, and quality all saw improvements. When compared to perovskites with a hydrophilic interlayer, those with a hydrophobic interlayer produced larger grain crystals with fewer grain boundaries, leading to better film coverage. Priyadarshini Karuppuswamy and colleagues used impedance spectroscopy to evaluate the effect of the pyrene layer on transport and recombination in PEDOT: PSS/$(CH_3NH_3)_3Sb_2I_9$ and Pyrene/$(CH_3NH_3)_3Sb_2I_9$ PSCs. Their discovery led them to the conclusion that pyrene prevented hysteresis in PSCs by reducing charge carrier recombination in $(CH_3NH_3)_3Sb_2I_9$. Researchers have shown that adding pyrene to solar cell materials makes them more efficient by allowing larger grains of Sb-based crystals to grow on the material. As a result, recombination near grain boundaries is less likely to occur (Karuppuswamy et al., 2018).

## 6.4 Semiconducting molecule outline

While creating inverted tin-based $FASnI_3$ perovskite in 2019, Cong Liu and colleagues added a semiconducting molecule known as poly [tetraphenylethene 3,3′-(((2,2-diphenylethene-1,1-diyl) bis(4,1-phenylene)) bis(oxy)) bis (N, N-diethylpropion-1amine) tetraphenylethene] (PTN-Br) into the perovskite precursor. A medium for transporting holes was established using the semiconducting molecule PTN-Br. It achieved this by filling the gaps between the grains at the grain borders. With a maximum occupied molecular orbital energy level of −5.41 eV, this molecule was selected. Additionally, Lewis adducts were formed when the dimethylamino group of PTNBr interacted with unattached Sn atoms. By interacting with the perovskite material, the π-conjugated polymer PTNBr was able to neutralize or deactivate trap states. Consequently, an efficiency of 7.14% was achieved. Integrating PTN-Br into the device increased its stability against UV radiation, thanks to the UV barrier and PTN-Br's passivating activity. It was able to preserve around 66% of its original efficiency even after being continuously exposed to UV light for 5 h (Liu C. et al., 2019). Therefore, the incorporation of semiconducting molecules enables the production of perovskite films with exceptional electrical properties.

## 6.5 Passivation surface

Bin Lyu et al. (2021) capped $CsSnCl_3$ perovskite nanocrystals (NC) with oleic acid/oleylamine (OA/OAm) using the hot injection technique. After that, the structural stability, optical responsiveness, durability, and eco-friendliness of these nanocrystals were improved by treating them with gelatin, a natural biomass material. The nanocrystals' performance was enhanced by the gelatin treatment, which enabled them to retain 77.4% of their photoluminescence intensity even after being distributed in water for 3 days. Polar solvents generate this effect by displacing the weaker amino-Sn coordination with the stronger carboxylate-Sn coordination. Nanocrystals bound to gelatin nevertheless exhibit mostly unaltered halogen-ammonium hydrogen bonding and carboxylate-Sn coordination. Additionally, gelatin has demonstrated anti-mildew properties that might find wider application (Lyu et al., 2021).

## 6.6 Alteration in the physical structure of the surface

The 2017 study by Biao Shi et al. utilized textured FTO substrates to create light-absorbing perovskites. The researchers

were able to increase the amount of light that could be absorbed and create larger grain-sized perovskite films with better charge transfer. Compared to smooth FTO substrates, textured FTO substrates significantly improved efficiency, reaching 22%. The short circuit density also increased significantly by 14.5 per cent. It follows that the surface form has a major impact on the enhanced efficacy of perovskites (Shi B. et al., 2017).

### 6.7 Lacking lead, perovskite quantum dots

Research indicates that perovskite quantum dots (PVQDs) are very suitable for optoelectronic devices (Wang et al., 2019c). Yangyang Wang and colleagues synthesized inorganic lead-free perovskite quantum dots $CsSnI_3$ using a one-pot synthesis using triphenyl phosphite (TPPi). This approach resulted in a remarkable efficiency of 5.03% for the quantum dots, and the devices made from them maintained a stable power conversion efficiency (PCE) for over 25 days (Shi B. et al., 2017). An improved hot-injection method was used by Hongzhe Xu et al. (2018) to create perovskite quantum dots with the composition $MASnBr_3$-xIx (x = 0, 1, 2, 3). Utilized as light absorbers in mesoscopic solar cells, these quantum dots attained an efficiency of 8.79% (Xu et al., 2018).

### 6.8 An introduction to chiral compounds

Pioneering research by Weiyin Gao et al., in 2022 showed how $FASnI_3$-based PSCs might be improved in hole transportation by utilizing chiral cations α-methylbenzylamine (S-/R-/rac-MBA). Aligning energy levels and facilitating effective charge transfer at the interface were both aided by the introduction of MBAs. To facilitate the targeted transfer of accumulated holes across interfaces, the chiral R-MBA cation set off the chiral-induced spin selectivity (CISS) phenomenon in R-$MBA_2SnI_4$. As a result, as mentioned in the reference, a power conversion efficiency (PCE) of 10.73% was achieved, along with improved device stability and reduced hysteresis (Gao et al., 2022).

### 6.9 Dion-Jacobson halide perovskites with low dimensions

Reducing Sn vacancies, improving stability with organic spacers, and perhaps increasing photo carrier transfer with divalent organic spacers were the outcomes of the synthesis of low-dimensional Dion-Jacobson Sn (II)-based halide perovskites carried out by Min Chen et al. (2018) (Chen et al., 2018c).

## 7 Conclusion

For PSCs to be extensively employed, breakthrough PVK materials that are extremely effective in light of electrical change, non-hazardous, and firm must be researched. The quest for novel PVK materials is anticipated to receive significantly expanded R&D funding during the next few years. While ongoing research towards this objective appears to develop rather randomly, we propose a reasonable roadmap that may help speed up R&D in this field. This road map is the first step toward understanding existing and future PVK noxiousness/dilapidation processes and advocates for more standardized experimental methodologies. After a comprehensive understanding of the toxicity/degradation pathways is achieved, innovative eco-friendly PVKs may be created that are particularly resistant to environmental stresses (using complementing theory-experiment techniques). Significant challenges are predicted for the future of lead-free stable PVKs thin-film manufacturing experiments in this paper. The latter is an essential step toward efficient and timely manufacturing of useful products. There are also promising new avenues for research into synthesis and processing that this opens. We anticipate that in the future, efficient and environmentally friendly PSCs will be realized because of this type of integrated scientific and technical R&D.

## Author contributions

SK: Conceptualization, Investigation, Writing–original draft, Writing–review and editing. SS: Conceptualization, Methodology, Writing–original draft, Writing–review and editing. JG: Conceptualization, Data curation, Investigation, Methodology, Writing–review and editing. EM: Conceptualization, Investigation, Methodology, Resources, Validation, Writing–review and editing. TS: Conceptualization, Investigation, Methodology, Validation, Writing–review and editing. HP: Conceptualization, Data curation, Investigation, Methodology, Writing–review and editing.

## Funding

The author(s) declare that no financial support was received for the research, authorship, and/or publication of this article.

## Conflict of interest

The authors declare that the research was conducted in the absence of any commercial or financial relationships that could be construed as a potential conflict of interest.

## Publisher's note

All claims expressed in this article are solely those of the authors and do not necessarily represent those of their affiliated organizations, or those of the publisher, the editors and the reviewers. Any product that may be evaluated in this article, or claim that may be made by its manufacturer, is not guaranteed or endorsed by the publisher.

# References


Abate, A. (2017). Perovskite solar cells go lead free. *Joule* 1, 659–664. doi:10.1016/j.joule.2017.09.007

Agresti, A., Pescetelli, S., Taheri, B., Del Rio Castillo, A. E., Cinà, L., Bonaccorso, F., et al. (2016). Graphene–perovskite solar cells exceed 18% efficiency: a stability study. *ChemSusChem* 9 (18), 2609–2619. doi:10.1002/cssc.201600942

Ali, R., Hou, G., Zhu, Z., Yan, Q., Zheng, Q., and Su, G. (2018a). Predicted lead-free perovskites for solar cells. *Chem. Mat.* 30, 718–728. doi:10.1021/acs.chemmater.7b04036

Ali, R., Hou, G. J., Zhu, Z. G., Yan, Q. B., Zheng, Q. R., and Su, G. (2018b). Predicted lead-free perovskites for solar cells. *J. Chem. Mater* 30, 718–728. doi:10.1021/acs.chemmater.7b04036

Ávila, J., Momblona, C., Boix, P. P., Sessolo, M., and Bolink, H. J. (2017). Vapor-deposited PVKs: the route to high-performance solar cell production? *Joule* 1, 431–442. doi:10.1016/j.joule.2017.07.014

Babayigit, A., Ethirajan, A., Muller, M., and Conings, B. (2016). Toxicity of organometal halide perovskite solar cells. *Nat. Mat.* 15, 247–251. doi:10.1038/nmat4572

Bai, F., Hu, Y., Hu, Y., Qiu, T., Miao, X., and Zhang, S. (2018). Lead-free, air-stable ultrathin Cs3Bi2I9 perovskite nanosheets for solar cells. *J. Sol. Energy Mater Sol. Cells* 184, 15–21. doi:10.1016/j.solmat.2018.04.032

Ball, J. M., Lee, M. M., Hey, A., and Snaith, H. J. (2013). Low-temperature processed meso-superstructured to thin-film perovskite solar cells. *Energy Environ. Sci.* 6 (6), 1739–1743. doi:10.1039/c3ee40810h

Ban, H., Zhang, T., Gong, X., Sun, Q., Zhang, X. L., Pootrakulchote, N., et al. (2021). Fully inorganic CsSnI 3 mesoporous perovskite solar cells with high efficiency and stability via coadditive engineering. *Sol. J. RRL* 5, 2100069. doi:10.1002/solr.202100069

Bansode, U., Naphade, R., Game, O., Agarkar, S., and Ogale, S. (2015). Hybrid perovskite films by a new variant of pulsed excimer laser deposition: a room-temperature dry process. *J. Phys. Chem. C* 119, 9177–9185. doi:10.1021/acs.jpcc.5b02561

Bi, D., Boschloo, G., Schwarzmüller, S., Yang, L., Johansson, E. M. J., and Hagfeldt, A. (2013). Efficient and stable CH3NH3PbI3-sensitized ZnO nanorod array solid-state solar cells. *Nanoscale* 5 (23), 11686–11691. doi:10.1039/c3nr01542d

Bonomi, S., Patrini, M., Bongiovanni, G., and Malavasi, L. (2020). Versatile vapor phase deposition approach to cesium tin bromide materials CsSnBr3, CsSn2Br5 and Cs2SnBr6. *J. RSC Adv.* 10, 28478–28482. doi:10.1039/d0ra04680a

Brunetti, B., Cavallo, C., Ciccioli, A., Gigli, G., and Latini, A. (2016). On the thermal and thermodynamic (In)Stability of methylammonium lead halide perovskites. *Sci. Rep.* 6, 31896. doi:10.1038/srep31896

Burschka, J., Pellet, N., Moon, S. J., Humphry Baker, R., Gao, P., Nazeeruddin, M. K., et al. (2013). Sequential deposition as a route to high-performance perovskite-sensitized solar cells. *Nature* 499, 316–319. doi:10.1038/nature12340

Cao, D. H., Stoumpos, C. C., Farha, O. K., Hupp, J. T., and Kanatzidis, M. G. (2015). 2D homologous perovskites as light-absorbing materials for solar cell applications. *J. Am. Chem. Soc.* 137, 7843–7850. doi:10.1021/jacs.5b03796

Castelli, I. E., Olsen, T., Datta, S., Landis, D. D., Dahl, S., Thygesen, K. S., et al. (2012). Computational screening of perovskite metal oxides for optimal solar light capture. *Energy Environ. Sci.* 5, 5814–5819. doi:10.1039/c1ee02717d

Chen, L. J., Lee, C. R., Chuang, Y. J., Wu, Z. H., and Chen, C. (2016b). Synthesis and optical properties of lead-free cesium tin halide perovskite quantum rods with high-performance solar cell application. *J. Phys. Chem. Lett.* 7, 5028–5035. doi:10.1021/acs.jpclett.6b02344

Chen, M., Gu, J., Sun, C., Zhao, Y., Zhang, R., You, X., et al. (2016a). Light-driven overall water splitting enabled by a photo-Dember effect realized on 3D plasmonic structures. *ACS Nano* 10, 6693–6701. doi:10.1021/acsnano.6b01999

Chen, M., Ju, M., Carl, A. D., Zong, Y., Grimm, R. L., Gu, J., et al. (2018b). Cesium titanium (IV) bromide thin films based stable lead-free perovskite solar cells. *J. Joule* 2, 558–570. doi:10.1016/j.joule.2018.01.009

Chen, M., Ju, M. G., Carl, A. D., Zong, Y., Grimm, R. L., Gu, J., et al. (2018a). Cesium titanium(IV) bromide thin films based stable lead-free PVK solar cells. *Joule* 2, 1–13. doi:10.1016/j.joule.2018.01.009

Chen, M., Ju, M. G., Garces, H. F., Carl, A. D., Ono, L. K., Hawash, Z., et al. (2019). Highly stable and efficient all-inorganic lead-free perovskite solar cells with native-oxide passivation. *J. Nat. Commun.* 10, 16. doi:10.1038/s41467-018-07951-y

Chen, M., Ju, M. G., Hu, M., Dai, Z., Hu, Y., Rong, Y., et al. (2018c). Lead-free dion-jacobson tin halide perovskites for photovoltaics. *J. ACS Energy Lett.* 4, 276–277. doi:10.1021/acsenergylett.8b02051

Christians, J. A., Fung, R. C. M., and Kamat, P. V. (2014). An inorganic hole conductor for organo-lead halide perovskite solar cells. improved hole conductivity with copper iodide. *J. Am. Chem. Soc.* 136 (2), 758–764. doi:10.1021/ja411014k

Chung, I., Song, J. H., Im, J., Androulakis, J., Malliakas, C. D., Li, H., et al. (2012). CsSnI3: semiconductor or metal? High electrical conductivity and strong near-infrared photoluminescence from a single material. High hole mobility and phase-transitions. *J. Am. Chem. Soc.* 134, 8579–8587. doi:10.1021/ja301539s

Coduri, M., Strobel, T. A., Szafra´nski, M., Katrusiak, A., Mahata, A., Cova, F., et al. (2019). Band gap engineering in MASnBr3 and CsSnBr3 perovskites: mechanistic insights through the application of pressure. *J. Phys. Chem. Lett.* 10, 7398–7405. doi:10.1021/acs.jpclett.9b03046

Correa-Baena, J. P., Saliba, M., Buonassisi, T., Gratzel, M., Abate, A., Tress, W., et al. (2017). Promises and challenges of perovskite solar cells. *Science* 358, 739–744. doi:10.1126/science.aam6323

Cortecchia, D., Dewi, H. A., Yin, J., Bruno, A., Chen, S., Baikie, T., et al. (2016). Lead-free $MA_2CuCl_xBr_{4-x}$ hybrid perovskites. *J. Inorg. Chem.* 55, 1044–1052. doi:10.1021/acs.inorgchem.5b01896

Cui, X., Jiang, K., Huang, J., Zhang, Q., Su, M., Yang, L., et al. (2015). Cupric bromide hybrid perovskite heterojunction solar cells. *J. Synth. Metall.* 209, 247–250. doi:10.1016/j.synthmet.2015.07.013

Dai, J., Ma, L., Ju, M., Huang, J., and Zeng, X. C. (2017). In- and Ga-based inorganic double perovskites with direct bandgaps for photovoltaic applications. *Phys. Chem. Chem. Phys.* 19, 21691–21695. doi:10.1039/c7cp03448b

Dai, Y., and Tüysüz, H. (2019). Lead-free Cs3Bi2Br9 perovskite as photocatalyst for ring opening reactions of epoxides. *J. Chem. Eur.* 12, 2587–2592. doi:10.1002/cssc.201900716

Dauvalter, V. (1955). Influence of pollution and acidification on metal concentrations in Finnish Lapland lake sediments. *Water Air Soil Pollut.* 85, 853–858. doi:10.1007/bf00476936

Dave, K., Fang, M. H., Bao, Z., Fu, H. T., and Liu, R. S. (2020). Recent developments in lead-free double perovskites: structure, doping, and applications. *J. Chem. Asian J.* 15, 242–252. doi:10.1002/asia.201901510

Debbichi, L., Lee, S., Cho, H., Rappe, A. M., Hong, K. H., Jang, M. S., et al. (2018). Mixed valence perovskite $Cs_2Au_2I_6$: a potential material for thin-film Pb-free photovoltaic cells with ultrahigh efficiency. *Adv. Mat.* 30, 1707001. doi:10.1002/adma.201707001

Diéguez, O., and Íñiguez, J. (2015). Epitaxial phases of BiMnO3 from first principles. *J. Phys. Rev. B* 91, 184113. doi:10.1103/physrevb.91.184113

Elumalai, N., Mahmud, M., Wang, D., and Uddin, A. (2016). Perovskite solar cells: progress and advancements. *Energies* 9 (11), 861. doi:10.3390/en9110861

Fabini, D. (2015). Quantifying the potential for lead pollution from halide perovskite photovoltaics. *J. Phys. Chem. Lett.* 6, 3546–3548. doi:10.1021/acs.jpclett.5b01747

Fang, D., Tong, Y., Xu, F., Mi, B., Cao, D., and Gao, Z. (2021). Preparation of CsSnBr3 perovskite film and its all-inorganic solar cells with planar heterojunction. *J. Solid State Chem.* 294, 121902. doi:10.1016/j.jssc.2020.121902

Florence, T. M., Lilley, S. G., and Stauber, J. L. (1988). Skin absorption of lead. *Lancet* 332, 157–158. doi:10.1016/s0140-6736(88)90702-7

Fu, H. (2019). Review of lead-free halide perovskites as light-absorbers for photovoltaic applications: from materials to solar cells. *J. Sol. Energy Mater Sol. Cells* 193, 107–132. doi:10.1016/j.solmat.2018.12.038

Fu, P. P., Xia, Q., Hwang, H. M., Ray, P. C., and Yu, H. (2014). Mechanisms of nanotoxicity: generation of reactive oxygen species. *J. Food Drug Anal.* 22, 64–75. doi:10.1016/j.jfda.2014.01.005

Ganose, A. M., Savory, C. N., and Scanlon, D. O. (2017). Beyond methylammonium lead iodide: prospects for the emergent field of ns2 containing solar absorbers. *J. Chemcomm.* 53, 20–44. doi:10.1039/c6cc06475b

Gao, W., Dong, H., Sun, N., Chao, L., Hui, W., Wei, Q., et al. (2022). Chiral cation promoted interfacial charge extraction for efficient tin-based perovskite solar cells. *J. Energy Chem.* 68, 789–796. doi:10.1016/j.jechem.2021.09.019

Gerber, G. B., and Léonard, A. (1997). Mutagenicity, carcinogenicity and teratogenicity of germanium compounds. *J. (MRR).* 387, 141–146. doi:10.1016/s1383-5742(97)00034-3

Ghosh, B., Wu, B., Mulmudi, H. K., Guet, C., Weber, K., Sum, T. C., et al. (2018). Limitations of Cs3Bi2I9 as lead-free photovoltaic absorber materials. *J. ACS Appl. Mat. Interfaces* 10, 35000–35007. doi:10.1021/acsami.7b14735

Ghrib, T., Rached, A., Algrafy, E., Al-nauim, I. A., Albalawi, H., Ashiq, M. G. B., et al. (2021). A new lead free double perovskites K2Ti(Cl/Br)6; a promising materials for optoelectronic and transport properties; probed by DFT. *J. Mat. Chem. Phys.* 264, 124435. doi:10.1016/j.matchemphys.2021.124435

Giustino, F., and Snaith, H. J. (2016). Toward lead-free perovskite solar cells. *ACS Energy Lett.* 1, 1233–1240. doi:10.1021/acsenergylett.6b00499

Grandhi, G. K., Matuhina, A., Liu, M., Annurakshita, S., Ali-L¨oytty, H., Bautista, G., et al. (2021). Lead-free cesium titanium bromide double perovskite nanocrystals. *J. Nanomater.* 11, 1458. doi:10.3390/nano11061458

Gratzel, M. (2014). The light and shade of perovskite solar cells. *Nat. Mat.* 13, 838–842. doi:10.1038/nmat4065

Green, M. A., Ho-Baillie, A., and Snaith, H. J. (2014). The emergence of perovskite solar cells. *Nat. Phot.* 8, 506–514. doi:10.1038/nphoton.2014.134

Greul, E., Docampo, P., and Bein, T. (2017). Synthesis of hybrid tin halide perovskite solar cells with less hazardous solvents: methanol and 1,4-dioxane. *J. Z Anorg. Allg. Chem.* 643, 1704–1711. doi:10.1002/zaac.201700297

Gu, F., Ye, S., Zhao, Z., Rao, H., Liu, Z., Bian, Z., et al. (2018). Improving performance of lead-free formamidinium tin triiodide perovskite solar cells by tin source purification. *J.Sol. RRL* 2, 1800136. doi:10.1002/solr.201800136

Gupta, S., Bendikov, T., Hodes, G., and Cahen, D. (2016). CsSnBr3, A lead-free halide perovskite for long-term solar cell application: insights on SnF2 addition. *J. ACS Energy Lett.* 1, 1028–1033. doi:10.1021/acsenergylett.6b00402

Hailegnaw, B., Kirmayer, S., Edri, E., Hodes, G., and Cahen, D. (2015). Rain on methylammonium lead iodide based perovskites: possible environmental effects of perovskite solar cells. *J. Phys. Chem. Lett.* 6, 1543–1547. doi:10.1021/acs.jpclett.5b00504

Handa, T., Yamada, T., Kubota, H., Ise, S., Miyamoto, Y., and Kanemitsu, Y. (2017). Photocarrier recombination and injection dynamics in long-term stable lead-free CH3NH3SnI3 perovskite thin films and solar cells. *J. Phys. Chem. C* 121, 16158–16165. doi:10.1021/acs.jpcc.7b06199

Haruyama, J., Sodeyama, K., Han, L., and Tateyama, Y. (2015). First-principles study of ion diffusion in perovskite solar cell sensitizers. *J. Am. Chem. Soc.* 137, 10048–10051. doi:10.1021/jacs.5b03615

Hebig, J., Kühn, I., Flohre, J., and Kirchartz, T. (2016). Optoelectronic properties of (CH3NH3) 3Sb2I9 thin films for photovoltaic applications. *J. ACS Energy Lett.* 1, 309–314. doi:10.1021/acsenergylett.6b00170

Heo, J. H., Kim, J., Kim, H., Moon, S. H., Im, S. H., and Hong, K. H. (2018). Roles of $SnX_2$ (X = F, Cl, Br) additives in tin-based halide perovskites toward highly efficient and stable lead-free perovskite solar cells. *J. Phys. Chem. Lett.* 9, 6024–6031. doi:10.1021/acs.jpclett.8b02555

Im, J. H., Jang, I. H., Pellet, N., Gratzel, M., and Park, N. G. (2014). Growth of CH3NH3PbI3 cuboids with controlled size for high-efficiency perovskite solar cells. *Nat. Nanotechnol.* 9, 927–932. doi:10.1038/nnano.2014.181

Jellicoe, T. C., Richter, J. M., Glass, H. F. J., Tabachnyk, M., Brady, R., Dutton, S. E., et al. (2016). Synthesis and optical properties of lead-free cesium tin halide perovskite nanocrystals. *J. Am. Chem. Soc.* 138, 2941–2944. doi:10.1021/jacs.5b13470

Jeon, N. J., Noh, J. H., Kim, Y. C., Yang, W. S., Ryu, S., and Seok, S. I. (2014). Solvent engineering for high-performance inorganic–organic hybrid perovskite solar cells. *Nat. Mat.* 13, 897–903. doi:10.1038/nmat4014

Jeon, N. J., Noh, J. H., Yang, W. S., Kim, Y. C., Ryu, S., Seo, J., et al. (2015). Compositional engineering of perovskite materials for high-performance solar cells. *Nature* 517 (7535), 476–480. doi:10.1038/nature14133

Jiang, F., Yang, D., Jiang, Y., Liu, T., Zhao, X., Ming, Y., et al. (2018). Chlorine-incorporation-induced Formation of the layered phase for antimony-based lead-free perovskite solar cells. *J. Am. Chem. Soc.* 140, 1019–1027. doi:10.1021/jacs.7b10739

Jokar, E., Chien, C. H., Tsai, C. M., Fathi, A., and Diau, E. W. G. (2018). Robust tin-based perovskite solar cells with hybrid organic cations to attain efficiency approaching 10. *J. Adv.Mater.* 31, 1804835. doi:10.1002/adma.201804835

Ju, M., Chen, M., Zhou, Y., Garces, H. F., Dai, J., Ma, L., et al. (2018). Earth-abundant nontoxic titanium(IV)-based vacancy-ordered double perovskite halides with tunable 1.0 to 1.8 eV bandgaps for photovoltaic applications. *J. ACS Energy Lett.* 3, 297–304. doi:10.1021/acsenergylett.7b01167

Ju, M. G., Dai, J., Ma, L., and Zeng, X. C. (2017a). Lead-free mixed tin and germanium perovskites for photovoltaic application. *J. Am. Chem. Soc.* 139, 8038–8043. doi:10.1021/jacs.7b04219

Ju, M. G., Dai, J., Ma, L., and Zeng, X. C. (2017b). Perovskite chalcogenides with optimal bandgap and desired optical absorption for photovoltaic devices. *Adv. Energy Mat.* 7, 1700216. doi:10.1002/aenm.201700216

Kalyanasundaram, K., and Grätzel, M. (1998). Applications of functionalized transition metal complexes in photonic and optoelectronic devices. *Coord. Chem. Rev.* 177 (1), 347–414. doi:10.1016/s0010-8545(98)00189-1

Kang, D., Liu, Q., Chen, M., Gu, J., and Zhang, D. (2016). Spontaneous cross-linking for fabrication of nanohybrids embedded with size-controllable particles fabrication of nanohybrids embedded with size-controllable particles. *ACS Nano* 10, 889–898. doi:10.1021/acsnano.5b06022

Karuppuswamy, P., Boopathi, K. M., Mohapatra, A., Chen, H., Wong, K., Wang, P., et al. (2018). Role of a hydrophobic scaffold in controlling the crystallization of methylammonium antimony iodide for efficient lead-free perovskite solar cells. *Nano Energy* 45, 330–336. doi:10.1016/j.nanoen.2017.12.051

Ke, W., and Kanatzidis, M. G. (2019). Prospects for low-toxicity lead-free perovskite solar cells. *J. Nat. Commun.* 10, 965. doi:10.1038/s41467-019-08918-3

Ke, W., Stoumpos, C. C., Spanopoulos, I., Mao, L., Chen, M., Wasielewski, M. R., et al. (2017b). Efficient Lead-Free Solar Cells Based on Hollow {en}MASnI3 Perovskites. *J. Am. Chem. Soc.* 139, 14800–14806. doi:10.1021/jacs.7b09018

Ke, W., Stoumpos, C. C., Zhu, M., Mao, L., Spanopoulos, I., Liu, J., et al. (2017a). Enhanced photovoltaic performance and stability with a new type of hollow 3D perovskite {en}$FASnI_3$. *Sci. Adv.* 3, e1701293. doi:10.1126/sciadv.1701293

Ke, W., Stoumpos, C. C., Zhu, M., Mao, L., Spanopoulos, I., Liu, J., et al. (2017c). Enhanced photovoltaic performance and stability with a new type of hollow 3D perovskite{en}FASnI 3. *J. Sci.Adv.* 3, 1701293. doi:10.1126/sciadv.1701293

Khalfin, S., and Bekenstein, Y. (2019). Advances in lead-free double perovskite nanocrystals, engineering band-gaps and enhancing stability through composition tunability. *J. Nanoscale* 11, 8665–8679. doi:10.1039/c9nr01031a

Kim, H. S., Lee, C. R., Im, J. H., Lee, K. B., Moehl, T., Marchioro, A., et al. (2012). Lead iodide perovskite sensitized all-solid-state submicron thin film mesoscopic solar cell with efficiency exceeding 9%. *Sci. Rep.* 2, 591. doi:10.1038/srep00591

Kim, Y., Yang, Z., Jain, A., Voznyy, O., Kim, G., Liu, M., et al. (2016). Pure cubic-phase hybrid iodobismuthates AgBi2I7 for thin-film photovoltaics. *J. Angew. Chem.* 128, 9738–9742. doi:10.1002/ange.201603608

Koh, T. M., Krishnamoorthy, T., Yantara, N., Shi, C., Leong, W. L., Boix, P. P., et al. (2015). Formamidinium tin-based perovskite with low Eg for photovoltaic applications. *J. Mat. Chem. A* 3, 14996–15000. doi:10.1039/c5ta00190k

Kojima, A., Teshima, K., Shirai, Y., and Miyasaka, T. (2009). Organometal halide perovskites as visible-light sensitizers for photovoltaic cells. *J. Am. Chem. Soc.* 131, 6050–6051. doi:10.1021/ja809598r

Kopacic, I., Friesenbichler, B., Hoefler, S. F., Kunert, B., Plank, H., Rath, T., et al. (2018). Enhanced performance of germanium halide perovskite solar cells through compositional engineering. *ACS Appl. Energy Mat.* 1, 343–347. doi:10.1021/acsaem.8b00007

Korbel, S., Marques, M. A. L., and Botti, S. (2016). Stability and electronic properties of new inorganic perovskites from high-throughput *ab initio* calculations. *J. Mat. Chem. C* 4, 3157–3167. doi:10.1039/c5tc04172d

Krishnamoorthy, T., Ding, H., Yan, C., Leong, W. L., Baikie, T., Zhang, Z., et al. (2015). Lead-free germanium iodide perovskite materials for photovoltaic applications. *J. Mat. Chem. A* 3, 23829–23832. doi:10.1039/c5ta05741h

Kulkarni, A., Singh, T., Ikegami, M., and Miyasaka, T. (2017). Photovoltaic enhancement of bismuth halide hybrid perovskite by N-methyl pyrrolidone-assisted morphology conversion. *J. RSC Adv.* 7, 9456–9460. doi:10.1039/c6ra28190g

Kumar, M. H., Dharani, S., Leong, W. L., Boix, P. P., Prabhakar, R. R., Baikie, T., et al. (2014). Lead-free halide perovskite solar cells with high photocurrents realized through vacancy modulation. *J. Adv. Mat.* 26, 7122–7127. doi:10.1002/adma.201401991

Lee, M. M., Teuscher, J., Miyasaka, T., Murakami, T. N., and Snaith, H. J. (2012). Efficient hybrid solar cells based on meso-superstructured organometal halide perovskites. *Science* 338, 643–647. doi:10.1126/science.1228604

Leijtens, T., Eperon, G. E., Noel, N. K., Habisreutinger, S. N., Petrozza, A., and Snaith, H. J. (2015). Stability of metal halide perovskite solar cells. *Adv. Energy Mat.* 5, 1500963. doi:10.1002/aenm.201500963

Leijtens, T., Eperon, G. E., Pathak, S., Abate, A., Lee, M. M., and Snaith, H. J. (2013). Overcoming ultraviolet light instability of sensitized TiO2 with meso-superstructured organometal tri-halide perovskite solar cells. *Nat. Commun.* 4, 2885. doi:10.1038/ncomms3885

Leijtens, T., Lauber, B., Eperon, G. E., Stranks, S. D., and Snaith, H. J. (2014). The importance of perovskite pore filling in organometal mixed halide sensitized TiO2-based solar cells. *J. Phys. Chem. Lett.* 5 (7), 1096–1102. doi:10.1021/jz500209g

Levin, S. M., Goldberg, M., and Doucette, J. T. (1997). The effect of the OSHA lead exposure in construction standard on blood lead levels among iron workers employed in bridge rehabilitation. *Am. J. Ind. Med.* 31, 303–309. doi:10.1002/(sici)1097-0274(199703)31:3<303::aid-ajim6>3.3.co;2-f

Li, B., Long, R., Xia, Y., and Mi, Q. (2018b). All-inorganic perovskite CsSnBr3 as a thermally stable, free-carrier semiconductor. *J. Angew. Chem. Int. Ed.* 57, 13154–13158. doi:10.1002/anie.201807674

Li, X., Wu, J., Wang, S., and Qi, Y. (2019). Progress of all-inorganic cesium lead-free perovskite solar cells. *J. Chem.Lett.* 48, 989–1005. doi:10.1246/cl.190270

Li, Z., Xu, Q., Sun, Q., Hou, Z., and Yin, W. (2018a). Stability engineering of halide PVK via machine learning. *ArXiv* 1803, 06042.

Liao, W., Zhao, D., Yu, Y., Grice, C. R., Wang, C., Cimaroli, A. J., et al. (2016). Lead-free inverted planar formamidinium tin triiodide perovskite solar cells achieving power conversion efficiencies up to 6.22%. *J. Adv. Mat.* 8, 9333–9340. doi:10.1002/adma.201602992

Liu, C., Li, W., Fan, J., and Mai, Y. (2018). A brief review on the lead element substitution in perovskite solar cells. *J. Energy Chem.* 27, 1054–1066. doi:10.1016/j.jechem.2017.10.028

Liu, C., Tu, J., Hu, X., Huang, Z., Meng, X., Yang, J., et al. (2019b). Enhanced hole transportation for inverted tin-based perovskite solar cells with high performance and stability. *J. Adv. Funct. Mat.* 29, 1808059. doi:10.1002/adfm.201808059

Liu, D., Peng, H., Zeng, H., and Sa, R. (2021). A promising all-inorganic double perovskite Rb2TiBr6 for photovoltaic applications: insight from first-principles calculations. *J. Solid State Chem.* 303, 122473. doi:10.1016/j.jssc.2021.122473

Liu, D., Zha, W., Yuan, R., Chen, J., and Sa, R. (2020b). A first-principles study on the optoelectronic properties of mixed-halide double perovskites Cs2TiI6 xBrx. *J. New J. Chem.* 44, 13613–13618. doi:10.1039/d0nj02535f

Liu, M., Johnston, M. B., and Snaith, H. J. (2013). Efficient planar heterojunction perovskite solar cells by vapour deposition. *Nature* 501, 395–398. doi:10.1038/nature12509

Liu, X., Wu, T., Chen, J.-Y., Meng, X., He, X., Noda, T., et al. (2020a). Templated growth of $FASnI_3$ crystals for efficient tin perovskite solar cells. *Energy Environ. Sci.* 13, 2896–2902. doi:10.1039/d0ee01845g

Liu, Y., Gao, Y., Zhi, J., Huang, R., Li, W., Huang, X., et al. (2022). Allinorganic lead-free NiOx/Cs3Bi2Br9 perovskite heterojunction photodetectors for ultraviolet multispectral imaging. *J. Nano Res.* 15, 1094–1101. doi:10.1007/s12274-021-3608-4

Liu, Y., Yang, C., Wang, M., Ma, X., and Yi, Y. (2019a). Theoretical insight into the optoelectronic properties of lead-free perovskite derivatives of Cs3Sb2X9 (X = Cl, Br, I). *J. Mat. Sci.* 54, 4732–4741. doi:10.1007/s10853-018-3162-y

Lozhkina, O. A., Murashkina, A. A., Shilovskikh, V. V., Kapitonov, Y. V., Ryabchuk, V. K., Emeline, A. V., et al. (2018). Invalidity of band-gap engineering concept for Bi3+ heterovalent doping in CsPbBr3 halide perovskite. *J. Phys. Chem. Lett.* 9, 5408–5411. doi:10.1021/acs.jpclett.8b02178

Lyu, B., Guo, X., Gao, D., Kou, M., Yu, Y., Ma, J., et al. (2021). Highly-stable tin-based perovskite nanocrystals produced by passivation and coating of gelatin. *J. Hazard Mat.* 403, 123967. doi:10.1016/j.jhazmat.2020.123967

Marshall, K. P., Walker, M., Walton, R. I., and Hatton, R. A. (2016). Enhanced stability and efficiency in hole-transport-layer-free CsSnI3 perovskite photovoltaics. *J. Nat.Energy* 1, 16178. doi:10.1038/nenergy.2016.178

Marshall, K. P., Walton, R. I., and Hatton, R. A. (2015). Tin perovskite/fullerene planar layer photovoltaics: improving the efficiency and stability of lead-free devices. *J. Mat. Chem.* 3, 11631–11640. doi:10.1039/C5TA02950C

McMeekin, D. P., Sadoughi, G., Rehman, W., Eperon, G. E., Saliba, M., Ho¨ rantner, M. T., et al. (2016). A mixed-cation lead mixed-halide perovskite absorber for tandem solar cells. *Science* 351, 151–155. doi:10.1126/science.aad5845

Meng, X., Liu, X., He, X., Noda, T., Han, L., Yang, X., et al. (2019). Highly stable and efficient FASnI 3-based perovskite solar cells by introducing hydrogen bonding. *J. Adv. Mat.* 31, 1903721. doi:10.1002/adma.201903721

Meng, X., Wang, Y., Lin, J., Liu, X., He, X., Barbaud, J., et al. (2020b). Surface-Controlled oriented growth of FASnI3 crystals for efficient lead-free perovskite solar cells. *Cells* 4, 902–912. doi:10.1016/j.joule.2020.03.007

Meng, X., Wu, T., Liu, X., He, X., Noda, X., Wang, T., et al. (2020a). Highly reproducible and efficient FASnI3 perovskite solar cells fabricated with volatilizable reducing solvent. *J. Phys. Chem. Lett.* 11, 2965–2971. doi:10.1021/acs.jpclett.0c00923

Ming, W., Shi, H., and Du, M. H. (2016). Large dielectric constant, high acceptor density, and deep electron traps in perovskite solar cell material $CsGeI_3$. *J. Mat. Chem. A* 4, 13852–13858. doi:10.1039/c6ta04685a

Moghe, D., Wang, L., Traverse, C. J., Redoute, A., Sponseller, M., Brown, P. R., et al. (2016). All vapor-deposited lead-free doped CsSnBr 3 planar solar cells. *J. Nano Energy* 28, 469–474. doi:10.1016/j.nanoen.2016.09.009

Nakajima, T., and Sawada, K. (2017). Discovery of Pb-free perovskite solar cells via high-throughput simulation on the K computer. *J. Phys. Chem. Lett.* 8, 4826–4831. doi:10.1021/acs.jpclett.7b02203

National Center for Photovoltaics (2024). *Best research-cell efficiencies*. U.S. Department of Energy, Office of Energy Efficiency and Renewable Energy. Available at: https://www.nrel.gov/pv/assets/images/efficiencychart.png.

Niu, G., Guo, X., and Wang, L. (2015). Review of recent progress in chemical stability of perovskite solar cells. *J. Mater Chem. A* 3, 8970–8980. doi:10.1039/c4ta04994b

Okamoto, Y., and Suzuki, Y. (2014). Perovskite-type SrTiO3, CaTiO3 and BaTiO3 porous film electrodes for dye-sensitized solar cells. *J. Ceram. Soc. Jpn.* 122, 728–731. doi:10.2109/jcersj2.122.728

Okano, T., and Suzuki, Y. (2017). Gas-assisted coating of Bi-based (CH3NH3) 3Bi2I9 active layer in perovskite solar cells. *J. Mat. Lett.* 191, 77–79. doi:10.1016/j.matlet.2017.01.047

Pang, S., Zhou, Y., Wang, Z., Yang, M., Krause, A. R., Zhou, Z., et al. (2016). Transformative evolution of organolead triiodide perovskite thin films from strong room-temperature solid–gas interaction between $HPbI_3$-$CH_3NH_2$ precursor pair. *J. Am. Chem. Soc.* 138, 750–753. doi:10.1021/jacs.5b11824

Patrick, C. E., Jacobsen, K. W., and Thygesen, K. S. (2015). Anharmonic stabilization and band gap renormalization in the PVK CsSnI3. *Phy. Rev. B* 92, 201205. doi:10.1103/physrevb.92.201205

Pilania, G., Balachandran, P. V., Kim, C., and Lookman, T. (2016). Finding new perovskite halides via machine learning. *Front. Mat.* 3, 19. doi:10.3389/fmats.2016.00019

Qin, P., Tanaka, S., Ito, S., Tetreault, N., Manabe, K., Nishino, H., et al. (2014). Inorganic hole conductor-based lead halide perovskite solar cells with 12.4% conversion efficiency. *Nat. Commun.* 5, 3834. doi:10.1038/ncomms4834

Qiu, X., Cao, B., Yuan, S., Chen, X., Qiu, Z., Jiang, Y., et al. (2017). From unstable CsSnI3 to air-stable Cs2SnI6: a lead-free perovskite solar cell light absorber with bandgap of 1.48 eV and high absorption coefficient. *J. Sol. Energy Mater Sol. Cells* 159, 227–234. doi:10.1016/j.solmat.2016.09.022

Ran, C., Wu, Z., Xi, J., Yuan, F., Dong, H., Lei, T., et al. (2017). Construction of compact methylammonium bismuth iodide film promoting lead-free inverted planar heterojunction organohalide solar cells with open-circuit voltage over 0.8 V. *J. Phys. Chem. Lett.* 8, 394–400. doi:10.1021/acs.jpclett.6b02578

Rong, Y., Liu, L., Mei, A., Li, X., and Han, H. (2015). Beyond efficiency: the challenge of stability in mesoscopic perovskite solar cells. *Adv. Energy Mat.* 5, 1501066. doi:10.1002/aenm.201501066

Sabba, D., Mulmudi, H. K., Prabhakar, R. R., Krishnamoorthy, T., Baikie, T., Boix, P. P., et al. (2015). Impact of anionic $Br^-$ substitution on open circuit voltage in lead free perovskite ($CsSnI_{3-x}Br_x$) solar cells. *J. Phys. Chem. C* 119, 1763–1767. doi:10.1021/jp5126624

Saha-Dasgupta, T. (2020). Double perovskites with 3d and 4d/5d transition metals: compounds with promises. *J. Mat. Res. Express* 7, 014003. doi:10.1088/2053-1591/ab6293

Sakai, N., Haghighirad, A. A., Filip, M. R., Nayak, P. K., Nayak, S., Ramadan, A., et al. (2017). Solutionprocessed cesium hexabromopalladate(IV), Cs2PdBr6, for optoelectronic applications. *J. Am. Chem. Soc.* 139, 6030–6033. doi:10.1021/jacs.6b13258

Sanders, S., Stümmler, D., Pfeiffer, P., Ackermann, N., Schimkat, F., Simkus, G., et al. (2018). Morphology control of organic–inorganic bismuth-based perovskites for solar cell application. *J. Phys. Status Solidi A* 215, 1800409. doi:10.1002/pssa.201800409

Sani, F., Shafie, S., Lim, H. N., and Musa, A. O. (2018). Advancement on lead-free organic-inorganic halide perovskite solar cells: a review. *J. Mat.* 11, 1008. doi:10.3390/ma11061008

Saparov, B., Hong, F., Sun, J. P., Duan, H. S., Meng, W., Cameron, S., et al. (2015). Thin-film preparation and characterization of $Cs_3Sb_2I_9$: a lead-free layered perovskite semiconductor. *Chem. Mat.* 27, 5622–5632. doi:10.1021/acs.chemmater.5b01989

Schauss, A. G. (1991). Nephrotoxicity and neurotoxicity in humans from organogermanium compounds and germanium dioxide. *J. Biol. Trace Elem. Res.* 29, 267–280. doi:10.1007/bf03032683

Schmidt, J., Shi, J., Borlido, P., Chen, L., Botti, S., and Marques, M. A. L. (2017). Predicting the thermodynamic stability of solids combining density functional theory and machine learning. *Chem. Mat.* 29, 5090–5103. doi:10.1021/acs.chemmater.7b00156

Shanon, R. D. (1976). Revised effective ionic radii and systematic studies of interatomic distances in halides and chalcogenides. *J. Acta Cryst.* 32, 751–767. doi:10.1107/s0567739476001551

Shao, S., Liu, J., Portale, G., Fang, H. H., Blake, G. R., Ten Brink, G. H., et al. (2017). Highly reproducible Sn-based hybrid perovskite solar cells with 9% efficiency. *J. Adv. Energy Mat.* 8, 1702019. doi:10.1002/aenm.201702019

Shi, B., Liu, B., Luo, J., Li, Y., Zheng, C., Yao, X., et al. (2017b). Enhanced light absorption of thin perovskite solar cells using textured substrates. *Sol. Energy Mat. Sol. Cells* 168, 214–220. doi:10.1016/j.solmat.2017.04.038

Shi, T., Zhang, H. S., Meng, W., Teng, Q., Liu, M., Yang, X., et al. (2017a). Effects of organic cations on the defect physics of tin halide perovskites. *J. Mat. Chem. A* 5, 15124–15129. doi:10.1039/C7TA02662E

Shtangeeva, I., Bali, R., and Harris, A. (2011a). Bioavailability and toxicity of antimony. *J. Geochem. Explor.* 110, 40–45. doi:10.1016/j.gexplo.2010.07.003

Shtangeeva, I., Bali, R., and Harris, A. (2011b). Bioavailability and toxicity of antimony. *J. Geochem. Explor.* 110, 40–45. doi:10.1016/j.gexplo.2010.07.003

Shum, K., Chen, Z., Qureshi, J., Yu, C. l., Wang, J. J., Pfenninger, W., et al. (2010). Synthesis and characterization of CsSnI3 thin films. *J. Phys. Lett.* 96, 221903. doi:10.1063/1.3442511

Singh, A., Boopathi, K. M., Mohapatra, A., Chen, Y. F., Li, G., and Chu, C. W. (2018). Photovoltaic performance of vapor-assisted solution-processed layer polymorph of Cs3Sb2I9. *J. ACS Appl. Mat. Interfaces* 10, 2566–2573. doi:10.1021/acsami.7b16349

Singh, T., Kulkarni, A., Ikegami, M., and Miyasaka, T. (2016). Effect of electron transporting layer on bismuth-based lead-free perovskite (CH3NH3)3 Bi2I9 for photovoltaic applications. *J. ACS Appl. Mat. Interfaces* 8, 14542–14547. doi:10.1021/acsami.6b02843

Slavney, A. H., Hu, T., Lindenberg, A. M., and Karunadasa, H. I. (2016). A bismuth-halide double perovskite with long carrier recombination lifetime for photovoltaic applications. *J. Am. Chem. Soc.* 138, 2138–2141. doi:10.1021/jacs.5b13294

Snaith, H. J. (2013). Perovskites: the emergence of a new era for low-cost, high-efficiency solar cells. *J. Phys. Chem. Lett.* 4, 3623–3630. doi:10.1021/jz4020162

Son, D. Y., Im, J. H., Kim, H. S., and Park, N. G. (2014). 11% efficient perovskite solar cell based on ZnO nanorods: an effective charge collection system. *J. Phys. Chem. C* 118 (30), 16567–16573. doi:10.1021/jp412407j

Song, T. B., Yokoyama, T., Aramaki, S., and Kanatzidis, M. G. (2017). Performance enhancement of lead-free tin-based perovskite solar cells with reducing atmosphere assisted dispersible additive. *J. ACS Energy Lett.* 2, 897–903. doi:10.1021/acsenergylett.7b00171

Song, T. B., Yokoyama, T., Logsdon, J., Wasielewski, M. R., Aramaki, S., and Kanatzidis, M. G. (2018). Piperazine suppresses self-doping in $CsSnI_3$ perovskite solar cells. *ACS Appl. Energy Mat.* 1, 4221–4226. doi:10.1021/acsaem.8b00866

Sun, P., Li, Q., Yang, L., and Li, Z. (2016). Theoretical insights into a potential lead-free hybrid perovskite: substituting Pb2+ with Ge2+. *J. Nanoscale* 8, 1503–1512. doi:10.1039/C5NR05337D

Sun, Q., and Yin, W. (2017). Thermodynamic stability trend of cubic perovskites. *J. Am. Chem. Soc.* 139, 14905–14908. doi:10.1021/jacs.7b09379

Takahashi, K., Takahashi, L., Miyazato, I., and Tanaka, Y. (2018). Searching for hidden perovskite materials for photovoltaic systems by combining data science and first principle calculations. *ACS Phot.* 5, 771–775. doi:10.1021/acsphotonics.7b01479

Tétreault, N., Horváth, E., Moehl, T., Brillet, J., Smajda, R., Bungener, S., et al. (2010). High efficiency solid-state dye-sensitized solar cells: fast charge extraction through self-assembled 3D fibrous network of crystalline TiO2 nanowires. *ACS Nano* 4, 7644–7650. doi:10.1021/nn1024434

Tsai, C. M., Mohanta, N., Wang, C. Y., Lin, Y. P., Yang, Y. W., Wang, C. L., et al. (2017). Formation of stable tin perovskites Co-crystallized with three halides for carbon-based mesoscopic lead-free perovskite solar cells. *Angew. Chem. Int. Ed.* 56, 13819–13823. doi:10.1002/anie.201707037

Tsai, H., Nie, W., Blancon, J. C., Stoumpos, C. C., Asadpour, R., Harutyunyan, B., et al. (2016). High-efficiency two-dimensional Ruddlesden–Popper perovskite solar cells. *Nature* 536, 312–316. doi:10.1038/nature18306

Umedov, S. T., Grigorieva, A. V., Lepnev, L. S., Knotko, A. V., Nakabayashi, K., hkoshi, S. I., et al. (2020). Indium doping of lead-free perovskite Cs2SnI6. *J. Front. Chem.* 8, 564. doi:10.3389/fchem.2020.00564

Volans, G. N. (1987). Medical toxicology, diagnosis and treatment of human poisoning. *Trends Pharmacol. Sci.* 9, 267. doi:10.1016/0165-6147(88)90162-9

Volonakis, G., and Giustino, F. (2018). Surface properties of lead-free halide double perovskites: possible visible-light photo-catalysts for water splitting. *J. Appl. Phys. Lett.* 112, 243901. doi:10.1063/1.5035274

Volonakis, G., Haghighirad, A. A., Milot, R. L., Sio, W. H., Filip, M. R., Wenger, B., et al. (2017). $Cs_2InAgCl_6$: a new lead-free halide double perovskite with direct band gap. *J. Phys. Chem. Lett.* 8, 772–778. doi:10.1021/acs.jpclett.6b02682

Wang, M., Zhang, T., Li, H., Ban, H., Sun, Q., and Shen, Y. (2020). Efficient CsSnI3-based inorganic perovskite solar cells based on mesoscopic metal oxide framework via incorporating donor element. *J. Mat. Chem.* doi:10.1039/C9TA11794F

Wang, N., Zhou, Y., Ju, M. G., Garces, H. F., Ding, T., Pang, S., et al. (2016). Heterojunction-depleted lead-free perovskite solar cells with coarse-grained B-γ-$CsSnI_3$ thin films. *Adv. Energy Mat.* 6, 1601130. doi:10.1002/aenm.201601130

Wang, X., Zhang, T., Lou, Y., and Zhao, Y. (2019a). All-inorganic lead-free perovskites for optoelectronic applications. *J. Mat. Chem. Front.* 3, 365–375. doi:10.1039/c8qm00611c

Wang, Y., Liu, Y., Xu, Y., Zhang, C., Bao, H., Wang, J., et al. (2019b). (CH3NH3)3Bi2I9 perovskite films fabricated via a two-stage electric-fieldassisted reactive deposition method for solar cells application. *J. Electrochim. Acta* 329, 135173. doi:10.1016/j.electacta.2019.135173

Wang, Y., Tu, J., Li, T., Tao, C., Deng, X., and Li, Z. (2019c). Convenient preparation of CsSnI3 quantum dots, excellent stability, and the highest performance of lead-free inorganic perovskite solar cells so far. *J. Mat. Chem. A* 7, 7683–7690. doi:10.1039/c8ta10901j

Wani, A. L., Ara, A., and Usmani, J. A. (2015). Lead toxicity: a review. *Interdiscip. Toxicol.* 8, 55–64. doi:10.1515/intox-2015-0009

Weber, S., Rath, T., Fellner, K., Fischer, R., Resel, R., Kunert, B., et al. (2019). Influence of the iodide to bromide ratio on crystallographic and optoelectronic properties of rubidium antimony halide perovskites. *J. ACS Appl. Energy Mat.* 2, 539–547. doi:10.1021/acsaem.8b01572

Wojciechowski, K., Saliba, M., Leijtens, T., Abate, A., and Snaith, H. J. (2014). Sub-150 °C processed meso-superstructured perovskite solar cells with enhanced efficiency. *Energy Environ. Sci.* 7 (3), 1142–1147. doi:10.1039/c3ee43707h

Wu, B., Zhou, Y., Xing, G., Xu, Q., Garces, H. F., Solanki, A., et al. (2017). Long minority-carrier diffusion length and low surface-recombination velocity in inorganic lead-free $CsSnI_3$ perovskite crystal for solar cells. *Adv. Funct. Mat.* 27, 1604818. doi:10.1002/adfm.201604818

Wu, C., Zhang, Q., Liu, Y., Luo, W., Guo, X., Huang, Z., et al. (2018). The dawn of lead-free perovskite solar cell: highly stable double perovskite Cs2AgBiBr6 film. *J. Adv. Sci.* 5, 1700759. doi:10.1002/advs.201700759

Xiao, J., Shi, J., Li, D., and Meng, Q. (2015b). Perovskite thin-film solar cell: excitation in photovoltaic science. *Sci. China Chem.* 58 (2), 221–238. doi:10.1007/s11426-014-5289-2

Xiao, Z., Cheng, B., Shao, Y., Dong, Q., Wang, Q., Yuan, Y., et al. (2014). Efficient, high yield perovskite photovoltaic devices grown by interdiffusion of solution-processed precursor stacking layers. *Energy Environ. Sci.* 7, 2619–2623. doi:10.1039/c4ee01138d

Xiao, Z., Du, K., Meng, W., Wang, J., Mitzi, D. B., and Yan, Y. (2017a). Intrinsic instability of $Cs_2In(I)M(III)X_6$ (M = Bi, Sb; X = halogen) double perovskites: a combined density functional theory and experimental study. *J. Am. Chem. Soc.* 139, 6054–6057. doi:10.1021/jacs.7b02227

Xiao, Z., Du, K. Z., Meng, W., Mitzi, D. B., and Yan, Y. (2017b). Chemical origin of the stability difference between copper(I)- and silver(I)-Based halide double perovskites. *Angew. Chem. Int. Ed.* 56, 12107–12111. doi:10.1002/anie.201705113

Xiao, Z., Zhou, Y., Hosono, H., and Kamiya, T. (2015a). Intrinsic defects in a photovoltaic perovskite variant $Cs_2SnI_6$. *Phys. Chem. Chem. Phys.* 17, 18900–18903. doi:10.1039/c5cp03102h

Xiao, Z., Zhou, Y., Hosono, H., Kamiya, T., and Padture, N. P. (2018). Bandgap optimization of perovskite semiconductors for photovoltaic applications. *Chemistry* 24, 2305–2316. doi:10.1002/chem.201705031

Xin, X., Scheiner, M., Ye, M., and Lin, Z. (2011). Surface-treated TiO2 nanoparticles for dye-sensitized solar cells with remarkably enhanced performance. *Langmuir* 27 (23), 14594–14598. doi:10.1021/la2034627

Xu, H., Yuan, H., Duan, J., Zhao, Y., Jiao, Z., and Tang, Q. (2018). Lead-free CH3NH3SnBr3-xIx perovskite quantum dots for mesoscopic solar cell applications. *Electrochim. Acta* 282, 807–812. doi:10.1016/j.electacta.2018.05.143

Yan, R., Chen, M., Zhou, H., Liu, T., Tang, X., Zhang, K., et al. (2016). Bio-inspired plasmonic nanoarchitectured hybrid system towards enhanced far red-to-near infrared solar photocatalysis. *Sci. Rep.* 6, 20001. doi:10.1038/srep20001

Yang, B., Chen, J., Hong, F., Mao, X., Zheng, K., Yang, S., et al. (2017). Lead-free, air-stable all-inorganic cesium bismuth halide perovskite nanocrystals. *Angew. Chem. Int. Ed.* 56, 12471–12475. doi:10.1002/anie.201704739

Yang, D., Zhang, G., Lai, R., Cheng, Y., Lian, Y., Rao, M., et al. (2021). Germanium-lead perovskite light-emitting diodes. *J. Nat. Commun.* 1, 4295. doi:10.1038/s41467-021-24616-5

Yin, Y., Huang, Y., Wu, Y., Chen, G., Yin, W. J., Wei, S. H., et al. (2017). Exploring emerging photovoltaic materials beyond perovskite: the case of skutterudite. *Chem. Mat.* 29, 9429–9435. doi:10.1021/acs.chemmater.7b03507

Zhang, C., Gao, L., Teo, S., Guo, Z., Xu, Z., Zhao, S., et al. (2018b). Design of a novel and highly stable lead-free Cs2NaBiI6 double perovskite for photovoltaic application. *J. Sustain. Energy Fuels* 2, 2419–2428. doi:10.1039/c8se00154e

Zhang, M., Lyu, M., Yun, J. H., Noori, M., Zhou, X., Cooling, N. A., et al. (2016a). Low-temperature processed solar cells with formamidinium tin halide perovskite/fullerene heterojunctions. *J. Nano Res.* 9, 1570–1577. doi:10.1007/s12274-016-1051-8

Zhang, Q., Hao, F., Li, J., Zhou, Y., Wei, Y., and Lin, H. (2018a). Science and Technology of Advanced Materials, Perovskite solar cells: must lead be replaced – and can it be done? *J. Sci. Technol. Adv. Mater* 19, 425–442. doi:10.1080/14686996.2018.1460176

Zhang, R., Wang, M., Wan, Z., Wu, Z., and Xiao, X. (2023). Laser direct writing based flexible solar energy harvester. *Res. Eng.* 19, 101314. doi:10.1016/j.rineng.2023.101314

Zhang, T., Dar, M. I., Li, G., Xu, F., Guo, N., Gratzel, M., et al. (2017). Bication lead iodide 2D perovskite component to stabilize inorganic α-$CsPbI_3$ perovskite phase for high-efficiency solar cells. *Sci. Adv.* 3, e1700841. doi:10.1126/sciadv.1700841

Zhang, X., Wu, G., Gu, Z., Guo, B., Liu, W., Yang, S., et al. (2016b). Active-layer evolution and efficiency improvement of $(CH_3NH_3)_3Bi_2I_9$-based solar cell on TiO2-deposited ITO substrate. *J. Nano Res.* 9, 2921–2930. doi:10.1007/s12274-016-1177-8

Zhao, X., Yang, D., Sun, Y., Li, T., Zhang, L., Yu, L., et al. (2017b). Cu–In halide perovskite solar absorbers. *J. Am. Chem. Soc.* 139, 6718–6725. doi:10.1021/jacs.7b02120

Zhao, X., Yang, J., Fu, Y., Yang, D., Xu, Q., Yu, L., et al. (2017a). Design of lead-free inorganic halide perovskites for solar cells via cation-transmutation. *J. Am. Chem. Soc.* 139, 2630–2638. doi:10.1021/jacs.6b09645

Zhou, Y., Zhou, Z., Chen, M., Zong, Y., Huang, J., Pang, S., et al. (2016). Doping and alloying for improved perovskite solar cells. *J. Mat. Chem. A* 4, 17623–17635. doi:10.1039/c6ta08699c

Zuo, C., and Ding, L. (2017). Lead-free perovskite materials $(NH_4)_3Sb_2I_xBr_{9-x}$. *J. Angew. Chem. Int. Ed.* 56, 6528–6532. doi:10.1002/anie.201702265

Zuo, L., Gu, Z., Ye, T., Fu, W., Wu, G., Li, H., et al. (2015). Enhanced photovoltaic performance of CH3NH3PbI3 perovskite solar cells through interfacial engineering using self-assembling monolayer. *J. Am. Chem. Soc.* 137 (7), 2674–2679. doi:10.1021/ja512518r